Max-Planck-Institut für Astrophysik

SFB-TR7

Excellence Cluster Universe

Quarks to Universe in Computational Science (QUCS 2012)
Nara, Japan, December 13–16

Nara Prefectural New Public Hall

Core-Collapse Supernovae

Unravelling the Explosion Mechanism by Computational Models

Hans-Thomas Janka
Max Planck Institute for Astrophysics, Garching

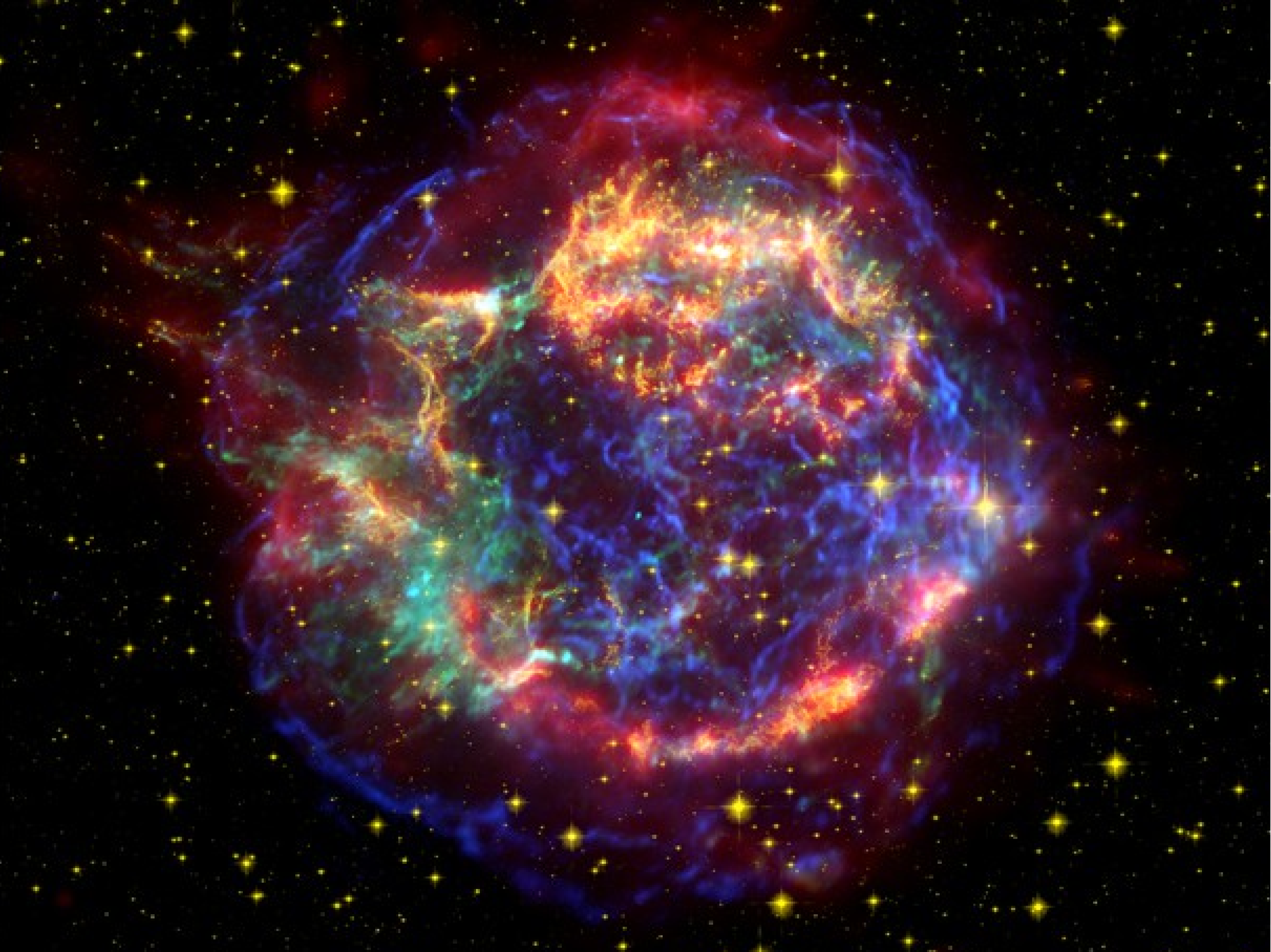

For concise reviews of most of what I will say, see

ARNPS 62 (2012) 407, arXiv:1206.2503
and
PTEP 2012, 01A309, arXiv:1211.1378

REVIEWS IN ADVANCE

Explosion Mechanisms of Core-Collapse Supernovae

Hans-Thomas Janka

Max Planck Institute for Astrophysics, D-85748 Garching, Germany;
email: thj@mpa-garching.mpg.de

Supernova and neutron star merger research is team effort

Students & postdocs:

Robert Bollig
Thomas Ertl
Tobias Melson
Andreas Voth

Florian Hanke
Lorenz Hüdepohl
Janina von Groote
Else Pllumbi
Tomasz Rembiasz

Andreas Bauswein
Oliver Just
Pedro Montero
Bernhard Müller
Marcella Ugliano
Annop Wongwathanarat

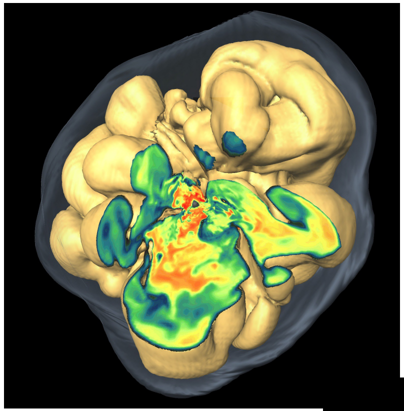

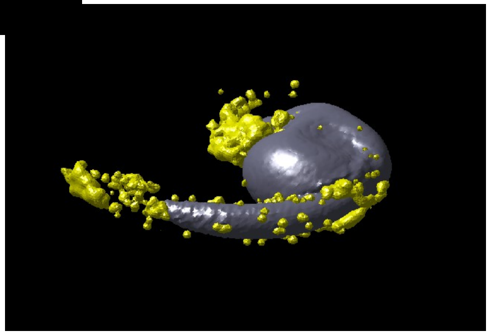

Collaborators:

Ewald Müller
Martin Obergaulinger
Andreas Marek
Stephane Goriely
Nick Stergioulas
Thomas Baumgarte
Georg Raffelt
Victor Utrobin
Shinya Wanajo

Outline

- Introduction to core-collapse supernova dynamics
- The neutrino-driven mechanism
- Status of self-consistent models in two dimensions
- The dimension conundrum: How does 3D differ from 2D?

Explosion Mechanism
by
Neutrino Heating

Evolved massive star prior to its collapse:

Star develops onion-shell structure in sequence of nuclear burning stages over millions of years

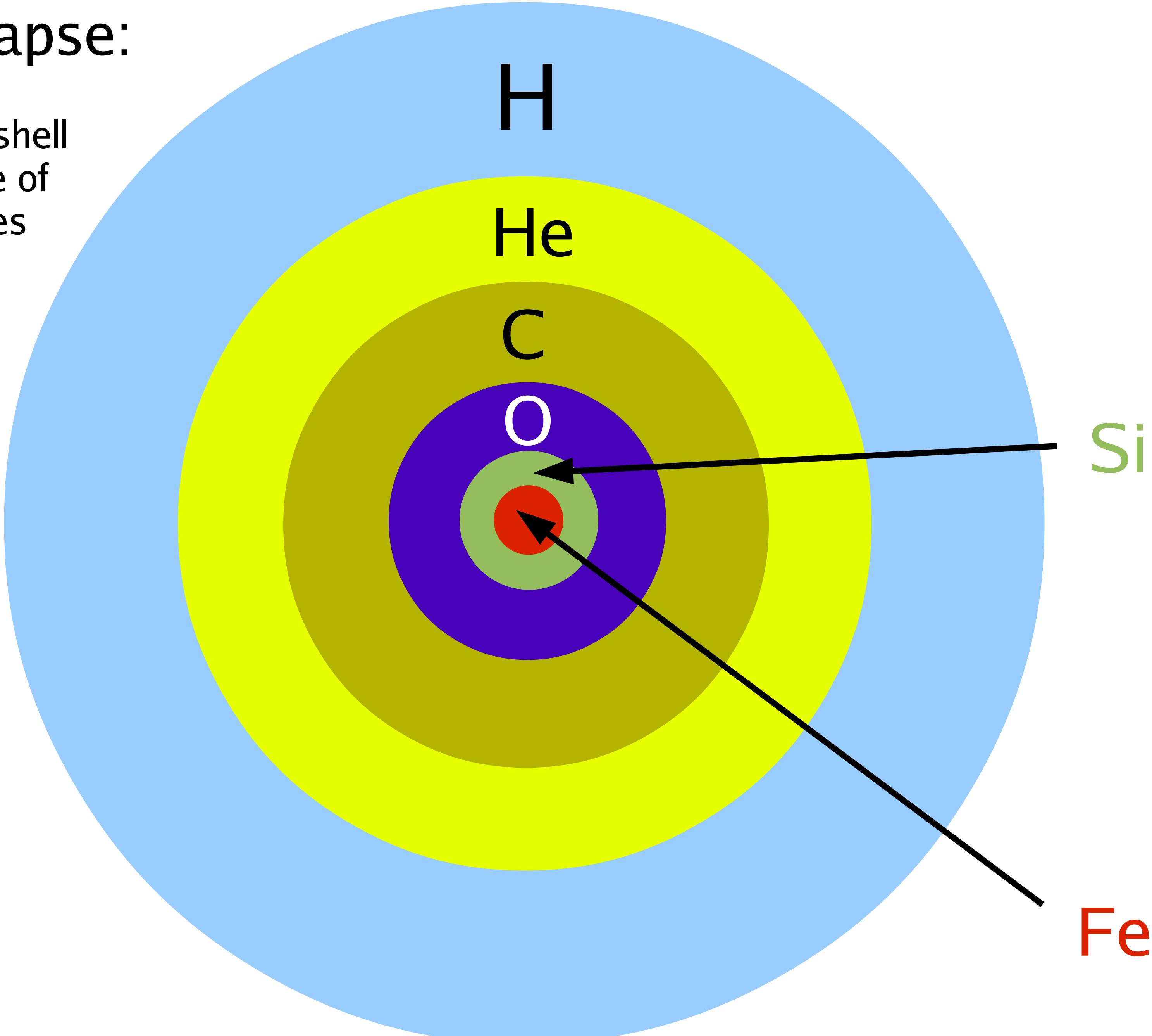

(layers not drawn to scale)

Evolved massive star prior to its collapse:

Star develops onion-shell structure in sequence of nuclear burning stages over millions of years

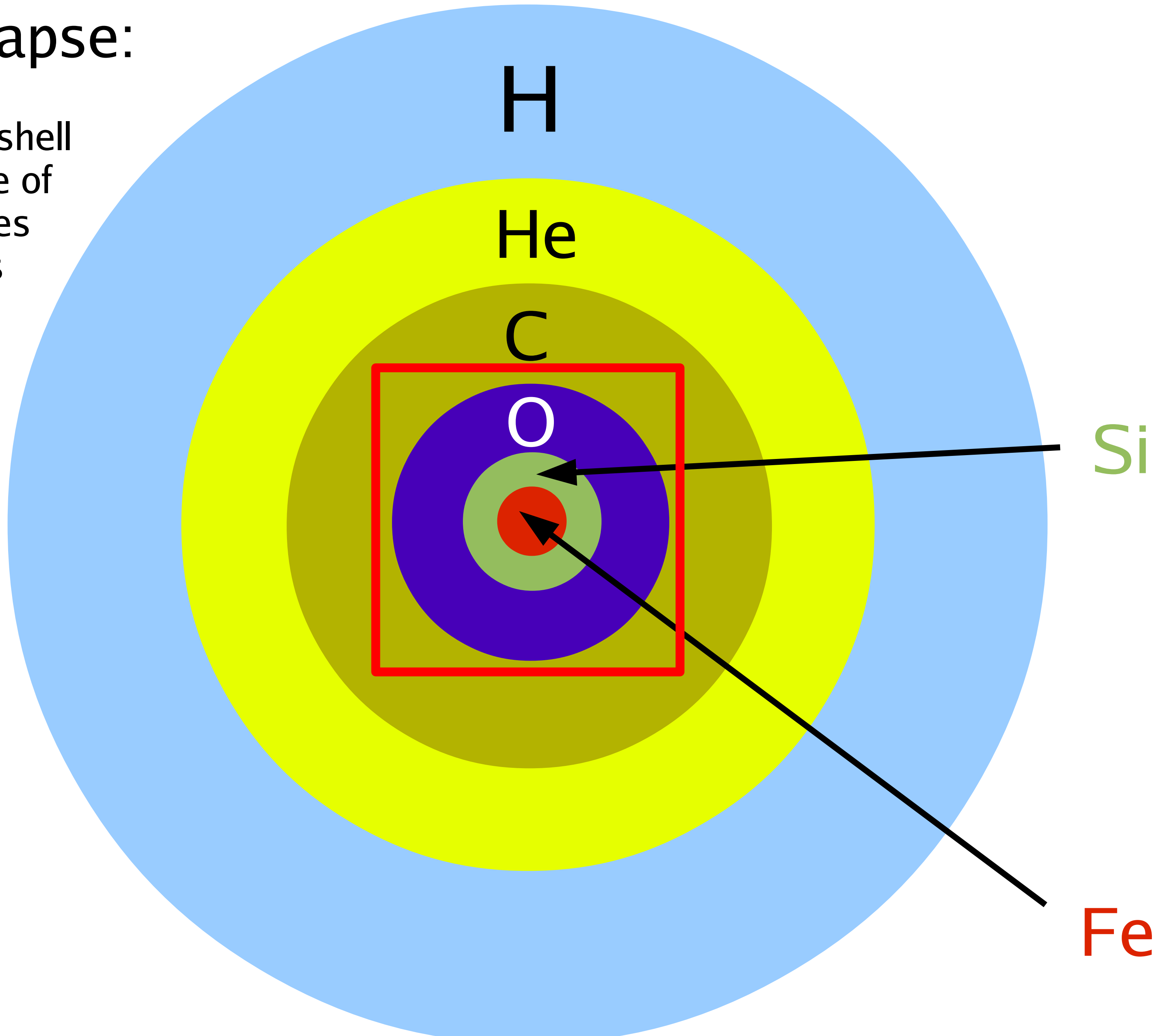

(layers not drawn to scale)

Gravitational instability of the stellar core:

Stellar iron core begins collapse when it reaches a mass near the critical Chandrasekhar mass limit

Collapse

becomes dynamical because of electron captures and photo-disintegration of Fe-group nuclei

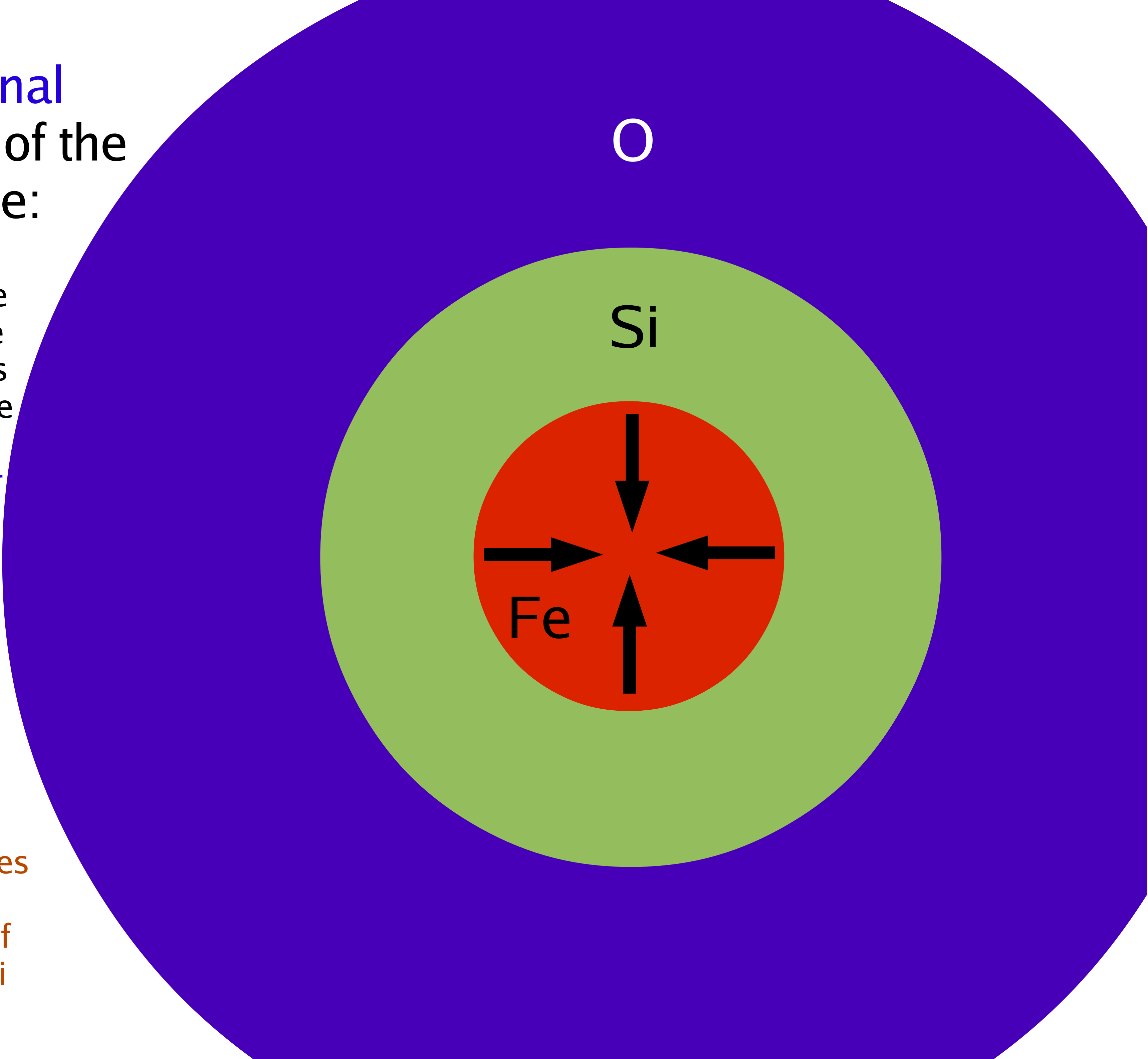

Core bounce at nuclear density:

Inner core bounces when nuclear matter density is reached and incompressibility increases

Shock wave forms

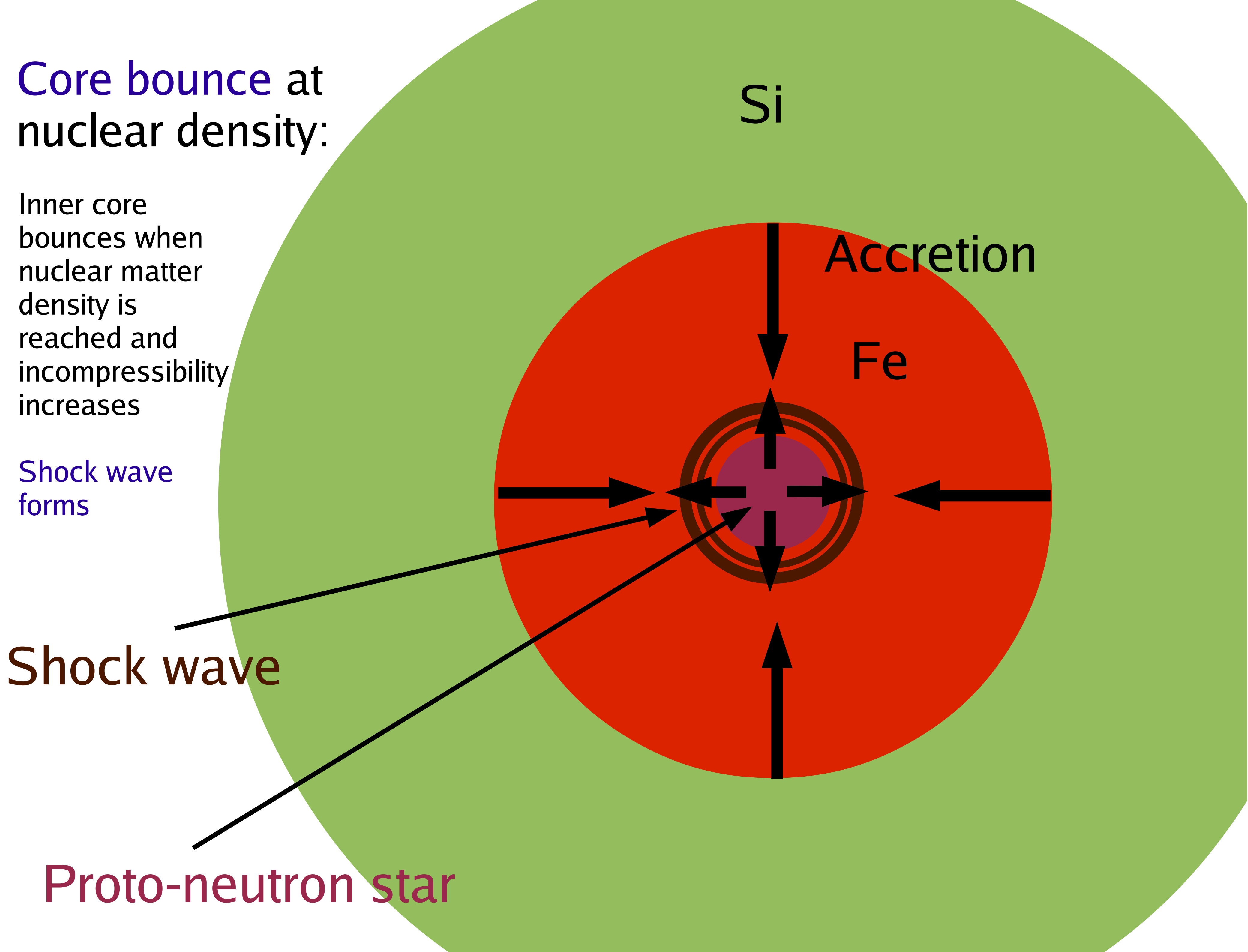

Shock stagnation:

Shock wave loses huge amounts of energy by photo-disintegration of Fe-group nuclei.

Shock stagnates still inside Fe-core

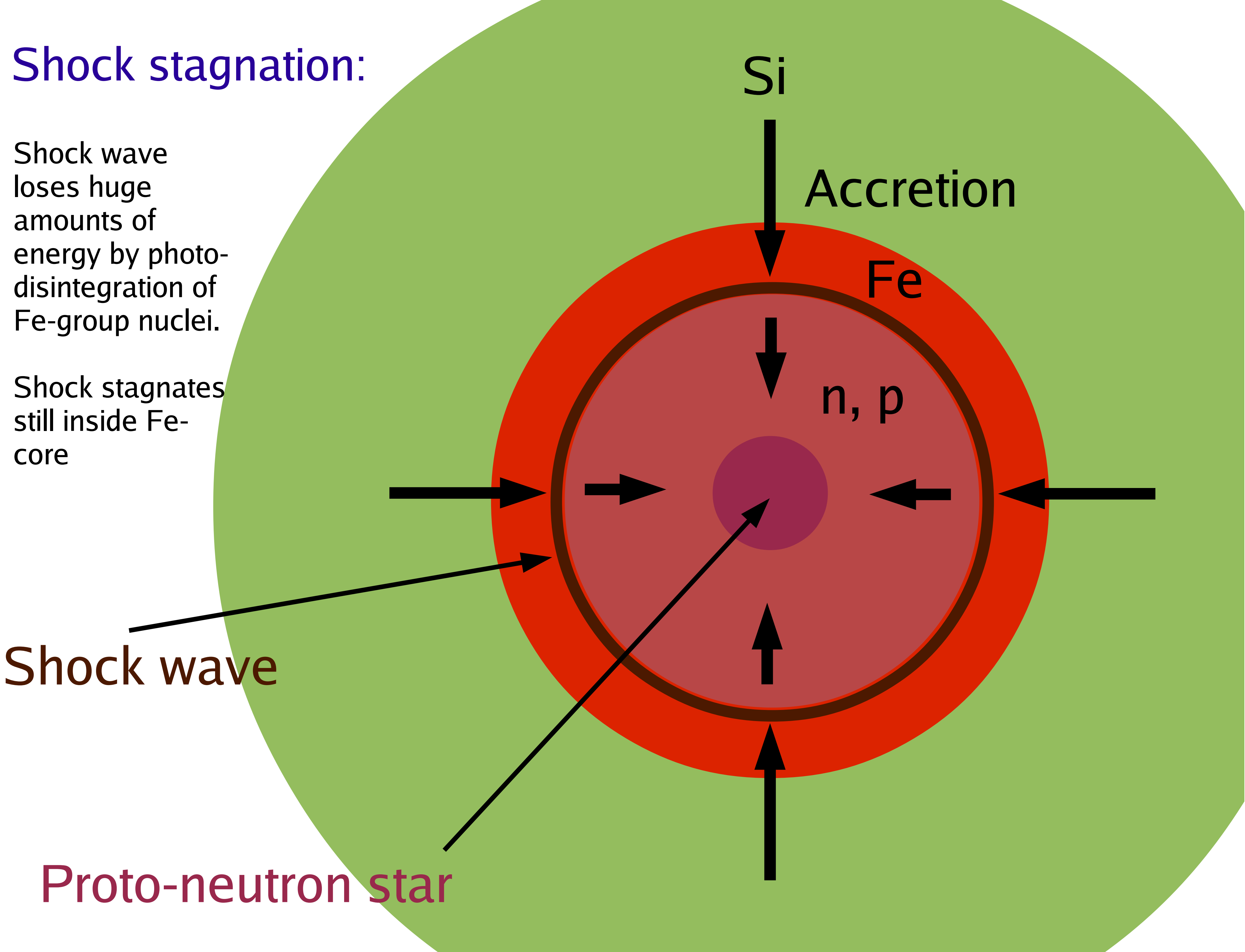

Shock “revival”:

Stalled shock wave must receive energy to start reexpansion against ram pressure of infalling stellar core.

Shock can receive fresh energy from neutrinos!

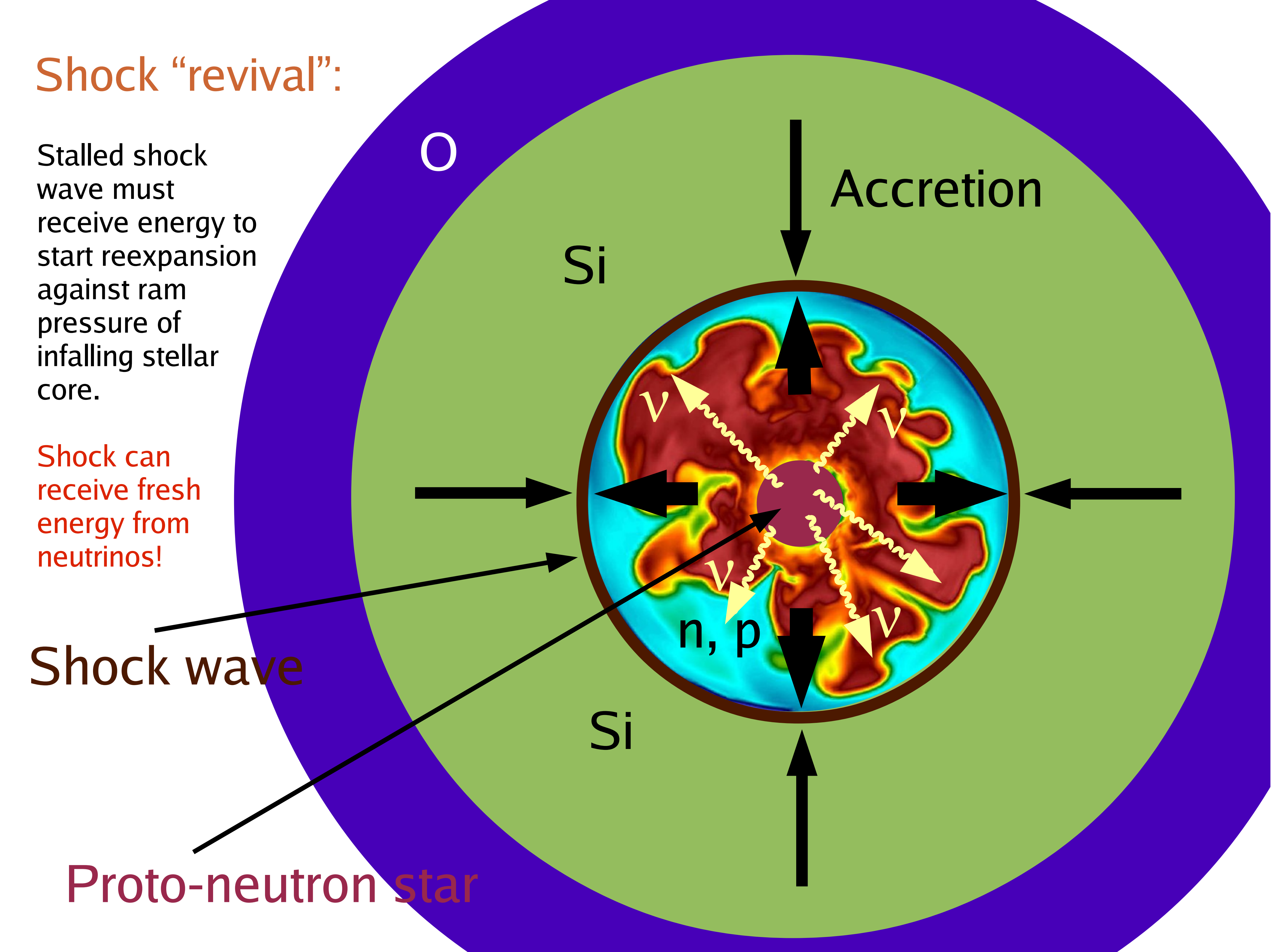

Explosion:

Shock wave expands into outer stellar layers, heats and ejects them.

Creation of radioactive nickel in shock-heated Si-layer.

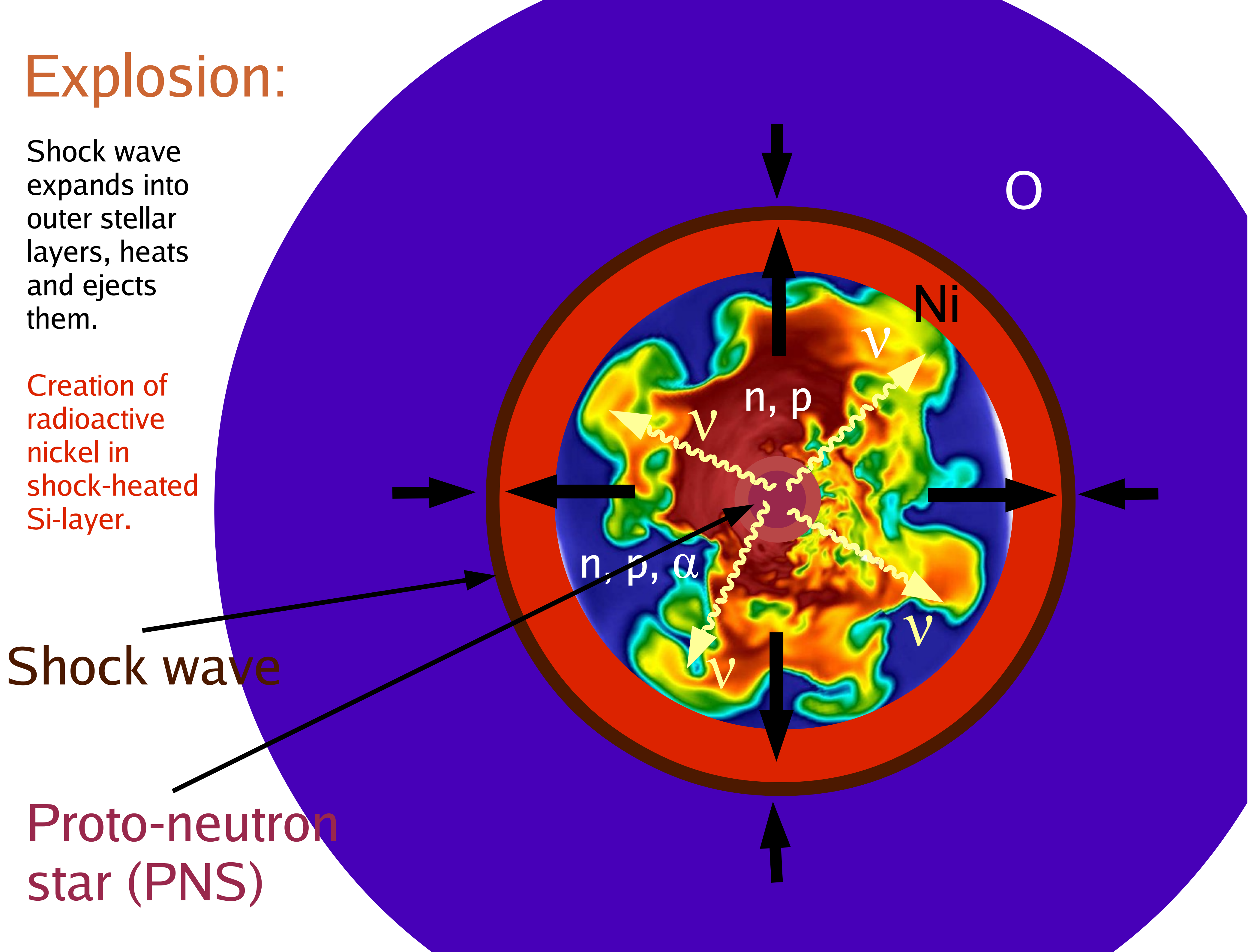

Nucleosynthesis during the explosion:

Shock-heated and neutrino-heated outflows are sites for element formation

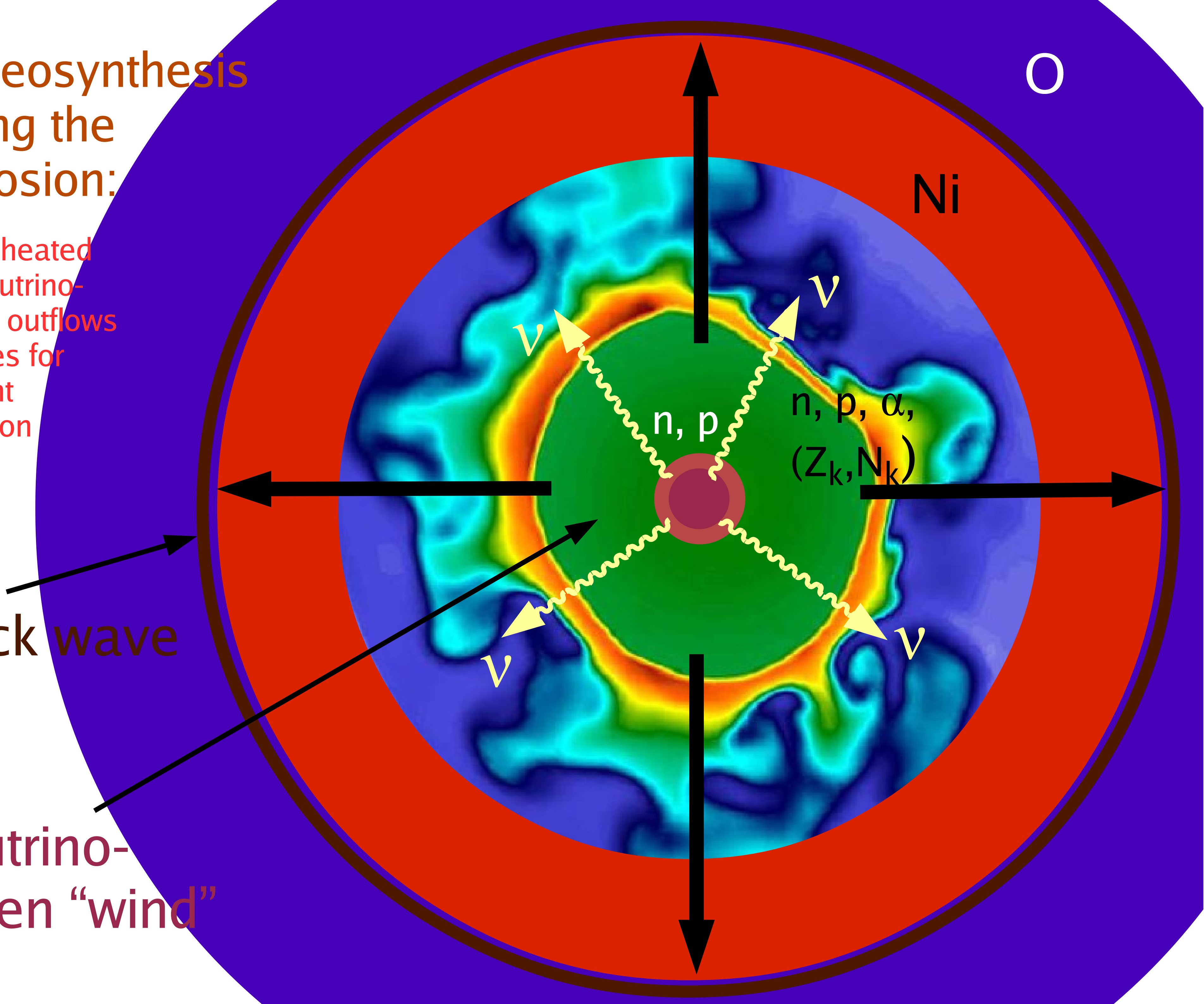

Neutrinos & SN Explosion Mechanism

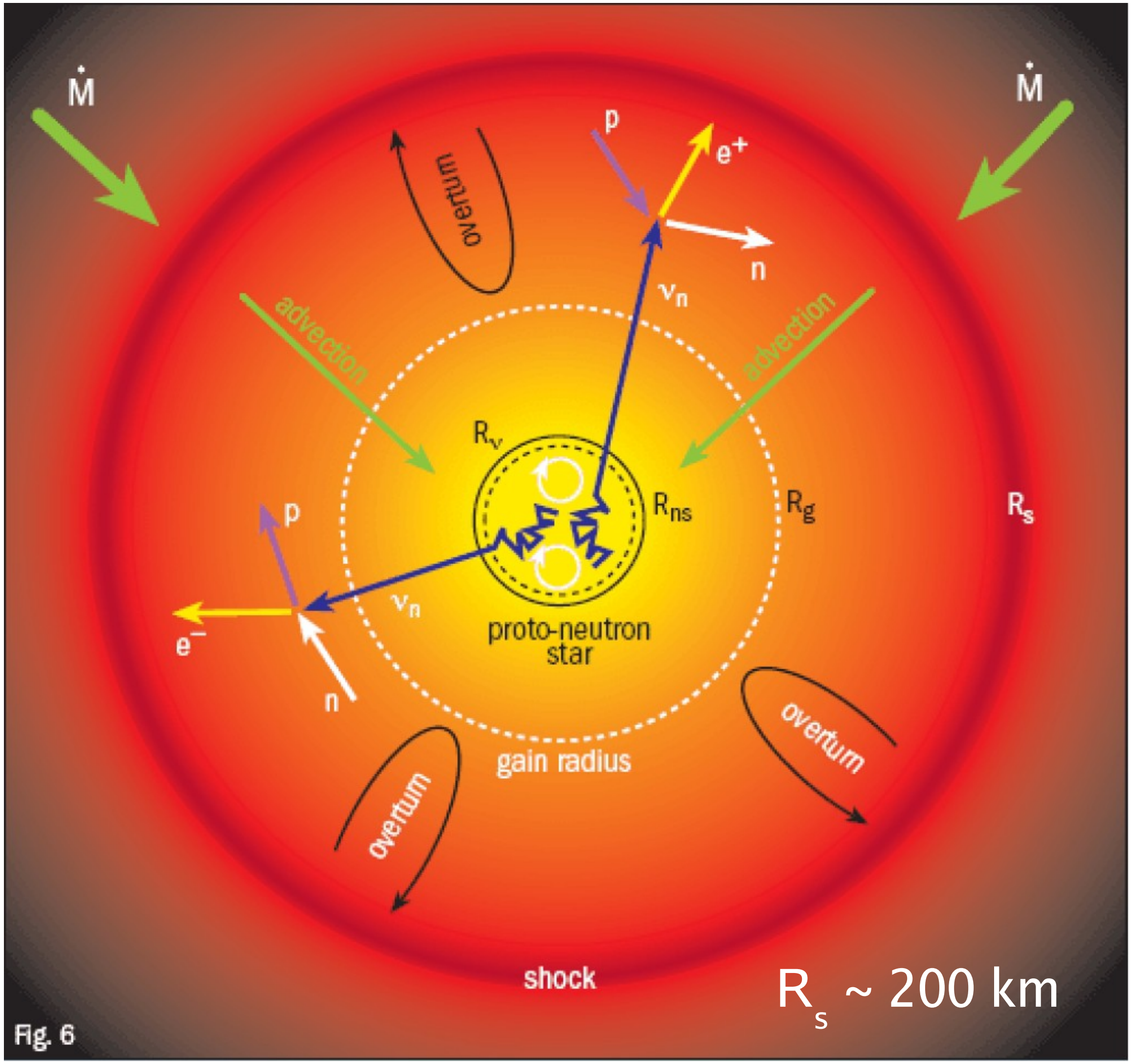

Paradigm: Explosions by the neutrino-heating mechanism, supported by hydrodynamic instabilities in the postshock layer

- "Neutrino-heating mechanism": Neutrinos `revive' stalled shock by energy deposition (Colgate & White 1966, Wilson 1982, Bethe & Wilson 1985);
- Convective processes & hydrodynamic instabilities support the heating mechanism (Herant et al. 1992, 1994; Burrows et al. 1995, Janka & Müller 1994, 1996; Fryer & Warren 2002, 2004; Blondin et al. 2003; Scheck et al. 2004,06,08, Iwakami et al. 2008, 2009, Ohnishi et al. 2006).

Neutrino Heating and Cooling

$$\boxed{\begin{aligned} \nu_e + n &\to e^- + p \\ \bar{\nu}_e + p &\to e^+ + n \end{aligned}}$$

- Neutrino heating:

$$q_\nu^+ = 1.544 \times 10^{20} \left(\frac{L_{\nu_e}}{10^{52}\ \mathrm{erg\ s^{-1}}}\right) \left(\frac{T_{\nu_e}}{4\ \mathrm{MeV}}\right)^2 \times \left(\frac{100\ \mathrm{km}}{r}\right)^2 (Y_n + Y_p) \qquad \left[\frac{\mathrm{erg}}{\mathrm{g\ s}}\right]$$

- Neutrino cooling:

$$\mathcal{C} = 1.399 \times 10^{20} \left(\frac{T}{2\ \mathrm{MeV}}\right)^6 (Y_n + Y_p) \qquad \left[\frac{\mathrm{erg}}{\mathrm{g\ s}}\right]$$

$$\begin{aligned} Q_\nu^+ &= q_\nu^+ M_g \\ &\sim 9.4 \times 10^{51} \frac{\mathrm{erg}}{\mathrm{s}} \left(\frac{k_B T_\nu}{4\ \mathrm{MeV}}\right)^2 \left(\frac{L_\nu}{3 \cdot 10^{52}\ \mathrm{erg/s}}\right) \left(\frac{M_g}{0.01\ M_\odot}\right) \left(\frac{R_g}{100\ \mathrm{km}}\right)^{-2} \end{aligned}$$

$$\boxed{\begin{aligned} E_N &\sim Q_\nu^+ t_{\mathrm{dwell}} \\ &\sim 9.4 \times 10^{50}\ \mathrm{erg} \left(\frac{k_B T_\nu}{4\ \mathrm{MeV}}\right)^2 \left(\frac{L_\nu}{3 \cdot 10^{52}\ \mathrm{erg/s}}\right) \times \\ &\quad \left(\frac{M_g}{0.01\ M_\odot}\right)^2 \left(\frac{\dot{M}}{0.1\ M_\odot\ \mathrm{s^{-1}}}\right)^{-1} \left(\frac{R_g}{100\ \mathrm{km}}\right)^{-2} \end{aligned}}$$

$$\boxed{t_{\mathrm{dwell}} \approx \frac{M_g}{\dot{M}}}$$

Hydrodynamic instabilities

See, e.g., Janka, ARNPS 62 (2012) 407

Supernova Explosion Energy

- Neutrino-energy deposition until onset of explosion makes postshock layer only marginally unbound: $E_{exp}(t_{exp}) \sim 0$

Additional energy by

- Recombination of nucleons to alpha particles and heavy nuclei in postshock matter ("recombination energy")
- Power of neutrino-driven wind on timescale of 1–2 seconds.
- Nuclear burning of shock-heated matter: Only small energy contribution because 0.1 M_{sun} of C+O —> Si, Ni yields $\sim 0.1 \times 10^{51}$ erg

- Negative energy contribution from gravitational binding energy of matter ahead of shock (and possible energy subtraction by fallback)

For a discussion, see Ugliano et al., ApJ 757 (2012) 69, and Scheck et al., A&A 457 (2006) 963.

Supernova Explosion Energy

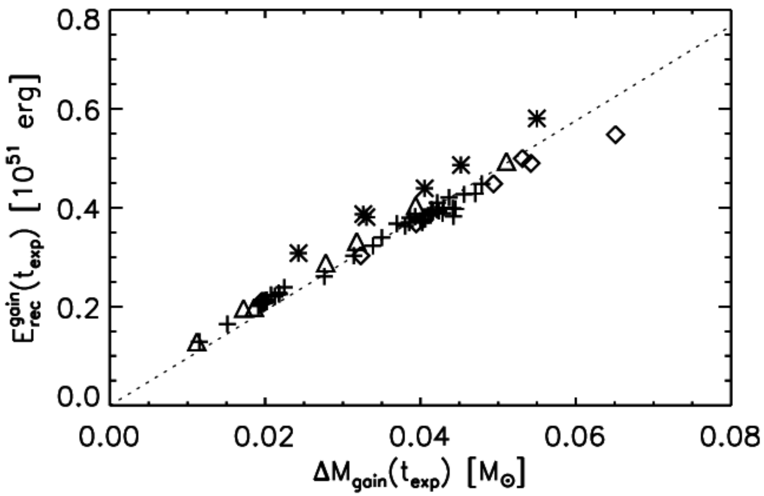

Fig. C.1. Available recombination energy, $E^{\rm gain}_{\rm rec}$, as a function of the mass in the gain layer, $\Delta M_{\rm gain}$, at the time of explosion for the models of Tables A.1–A.5. The slope of this approximately linear relation corresponds to about 5 MeV per baryon (dotted line).

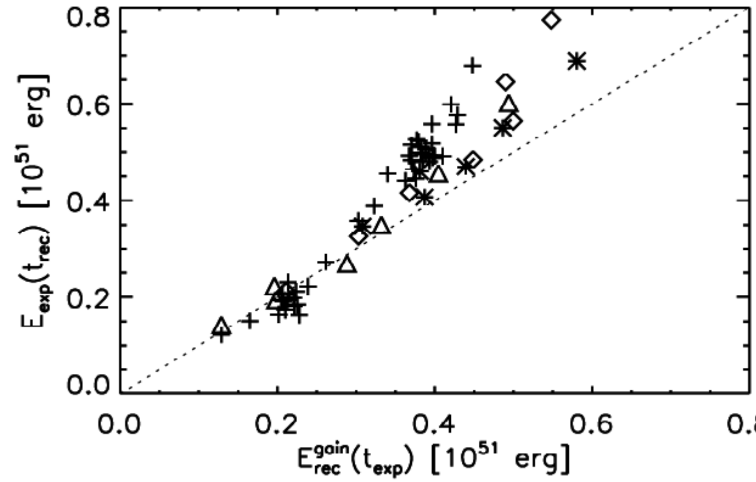

Fig. C.2. Explosion energy after the recombination of the ejecta, $E_{\rm exp}(t_{\rm rec})$, as a function of the available recombination energy in the gain layer at the onset of the explosion, $E^{\rm gain}_{\rm rec}(t_{\rm exp})$, for the models of Tables A.1–A.5. For low explosion energies the two quantities agree well.

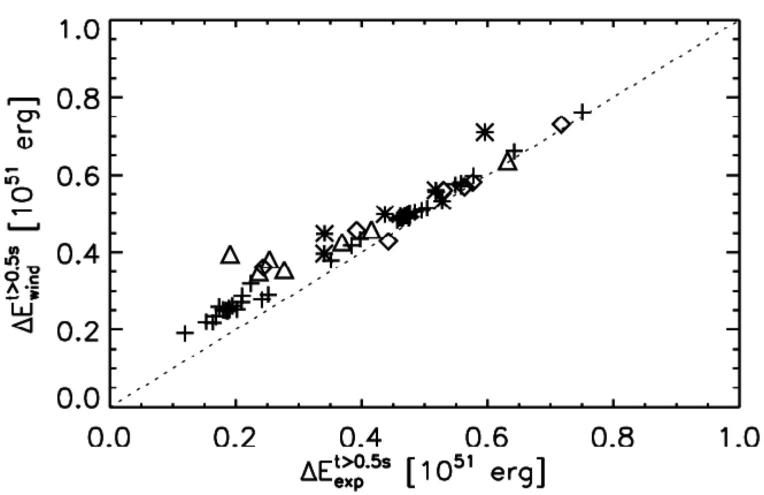

Fig. C.4. Relation between the increase of the explosion energy between $t = 0.5$ s and $t = 1$ s, $\Delta E^{t>0.5\,{\rm s}}_{\rm exp}$, and the integrated wind power during this time interval, $\Delta E^{t>0.5\,{\rm s}}_{\rm wind}$, for the models of Tables A.1–A.5.

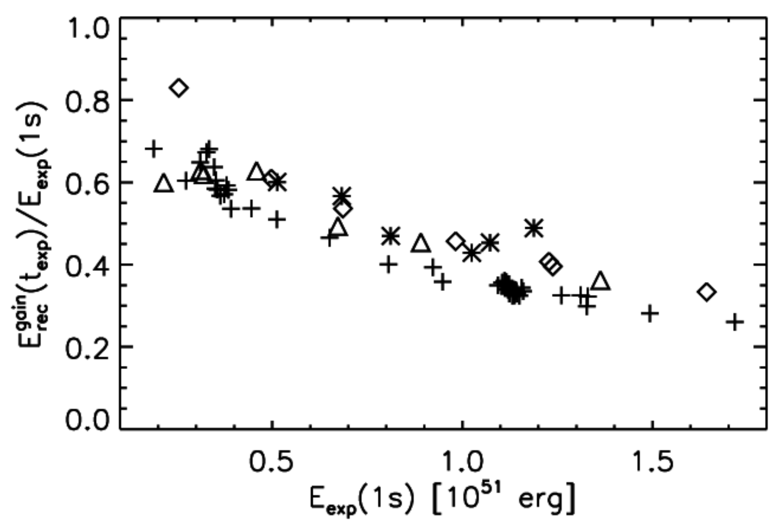

Fig. C.5. Ratio of the recombination contribution to the total explosion energy 1 s after core bounce, $E^{\rm gain}_{\rm rec}(t_{\rm exp})/E_{\rm exp}(1\,{\rm s})$, as a function of $E_{\rm exp}(1\,{\rm s})$ for the models of Tables A.1–A.5. For low-energy models the recombination contribution dominates, whereas for higher explosion energies the wind contribution becomes more important.

Scheck et al., A&A 457 (2006) 963

Possible additional evidence for neutrino-driven mechanism:

* Neutron star kicks
* Large-scale mixing instabilities

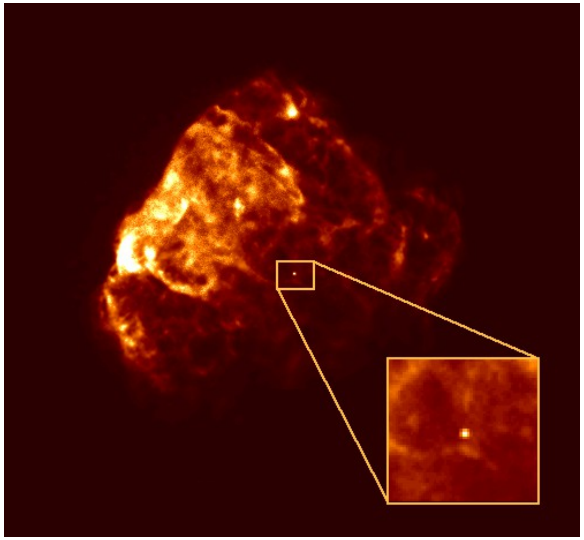

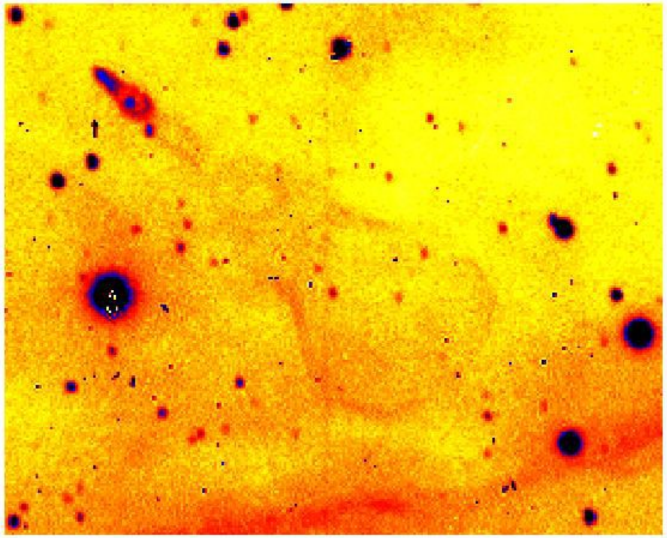

Neutron Star Kicks in 3D SN Explosions

Parametric —not fully self-consistent— explosion simulations:

Neutrino core luminosity of proto-NS chosen;
Accretion luminosity calculated with simple (grey) transport scheme

Neutron Star Recoil in 3D Explosion Models

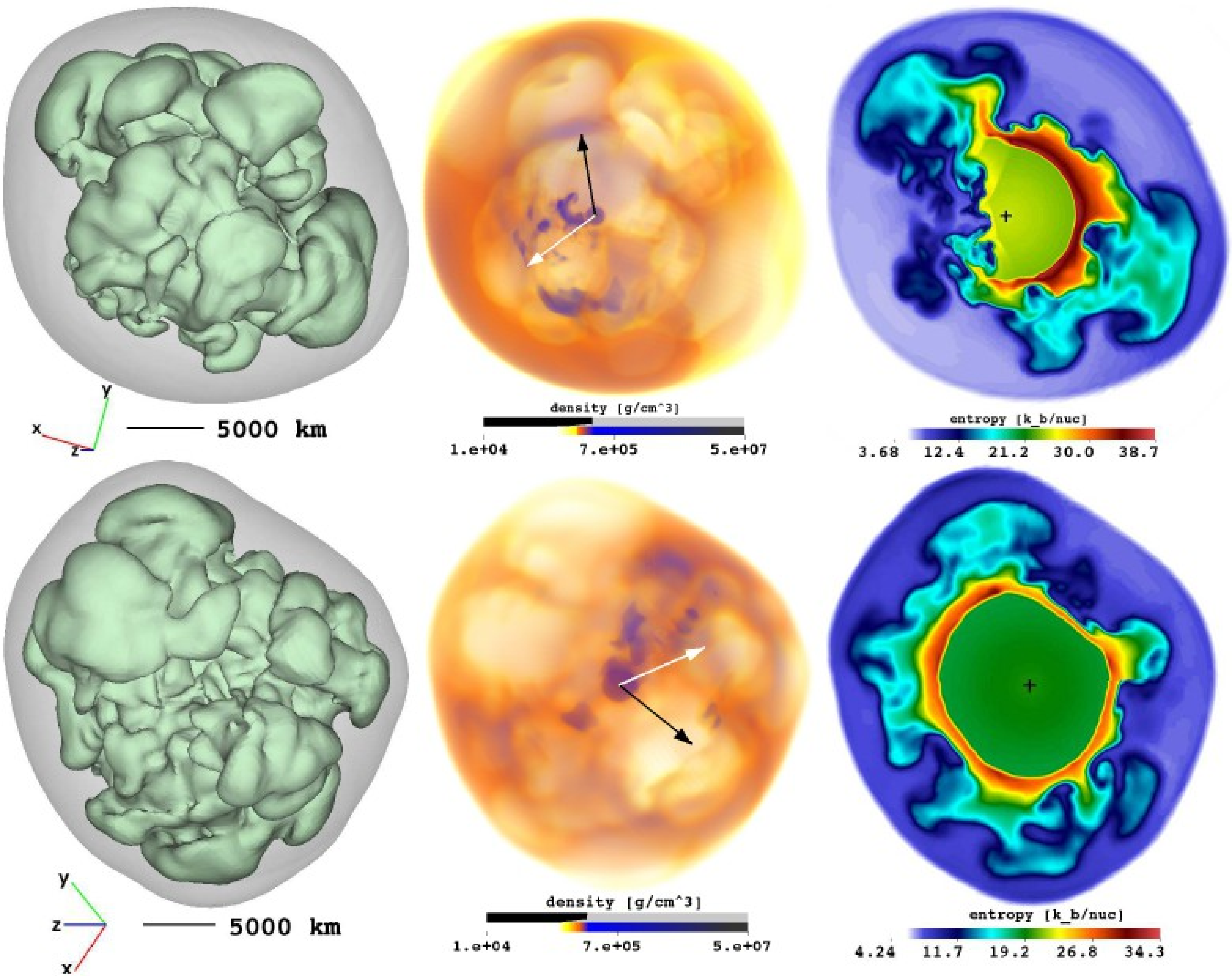

(Wongwathanarat, Janka, Müller, ApJL 725 (2010) 106; A&A, submitted, arXiv:1210.8148)

Neutron Star Recoil by "Gravitational Tug-Boat" Mechanism

@ t = 1.4 s   @ t = 3.3 s

Model	M_{ns} $[M_\odot]$	t_{exp} [ms]	E_{exp} [B]	v_{ns} [km/s]	a_{ns} [km/s^2]	$v_{ns,\nu}$ [km/s]	$\alpha_{k\nu}$ [°]	v_{ns}^{long} [km/s]	a_{ns}^{long} [km/s^2]	$J_{ns,46}$ [10^{46} g cm^2/s]	α_{sk} [°]	T_{spin} [ms]
W15-1	1.37	246	1.12	331	167	2	151	524	44	1.51	117	652
W15-2	1.37	248	1.13	405	133	1	126	575	49	1.56	58	632
W15-3	1.36	250	1.11	267	102	1	160	-	-	1.13	105	864
W15-4	1.38	272	0.94	262	111	4	162	-	-	1.27	43	785
W15-5-lr	1.41	289	0.83	373	165	2	129	-	-	1.63	28	625
W15-6	1.39	272	0.90	437	222	2	136	704	71	0.97	127	1028
W15-7	1.37	258	1.07	215	85	1	81	-	-	0.45	48	2189
W15-8	1.41	289	0.72	336	168	3	160	-	-	4.33	104	235
L15-1	1.58	422	1.13	161	69	5	135	227	16	1.89	148	604
L15-2	1.51	382	1.74	78	14	1	150	95	4	1.04	62	1041
L15-3	1.62	478	0.84	31	27	1	51	-	-	1.55	123	750
L15-4-lr	1.64	502	0.75	199	123	4	120	-	-	1.39	93	846
L15-5	1.66	516	0.62	267	209	3	147	542	106	1.72	65	695
N20-1-lr	1.40	311	1.93	157	42	7	118	-	-	5.30	122	190
N20-2	1.28	276	3.12	101	12	4	159	-	-	7.26	43	127
N20-3	1.38	299	1.98	125	15	5	138	-	-	4.42	54	225
N20-4	1.45	334	1.35	98	18	1	98	125	9	2.04	45	512
B15-1	1.24	164	1.25	92	16	1	97	102	1	1.03	155	866
B15-2	1.24	162	1.25	143	37	1	140	-	-	0.12	162	7753
B15-3	1.26	175	1.04	85	19	1	24	99	3	0.44	148	2050

(Wongwathanarat, Janka, Müller, ApJL 725 (2010) 106; A&A, to be submitted)

Neutron Star Recoil by "Gravitational Tug-Boat" Mechanism

@ t = 1.4 s   @ t = 3.3 s

Model	M_{ns} $[M_\odot]$	t_{exp} [ms]	E_{exp} [B]	v_{ns} [km/s]	a_{ns} [km/s^2]	$v_{ns,\nu}$ [km/s]	$\alpha_{k\nu}$ [°]	v_{ns}^{long} [km/s]	a_{ns}^{long} [km/s^2]	$J_{ns,46}$ [10^{46} g cm^2/s]	α_{sk} [°]	T_{spin} [ms]
W15-1	1.37	246	1.12	331	167	2	151	524	44	1.51	117	652
W15-2	1.37	248	1.13	405	133	1	12[illegible]	575	49	1.56	58	632
W15-3	1.36	250	1.11	267	102	1	160	-	-	1.13	105	864
W15-4	1.38	272	0.94	262	111	4	162	-	-	1.27	43	785
W15-5-lr	1.41	289	0.83	373	165	2	12[illegible]	-	-	1.63	28	625
W15-6	1.39	272	0.90	437	222	2	136	704	71	0.97	127	1028
W15-7	1.37	258	1.07	215	85	1	81	-	-	0.45	48	2189
W15-8	1.41	289	0.72	336	168	3	160	-	-	4.33	104	235
L15-1	1.58	422	1.13	161	69	5	135	227	16	1.89	148	604
L15-2	1.51	382	1.74	78	14	1	150	95	4	1.04	62	1041
L15-3	1.62	478	0.84	31	27	1	51	-	-	1.55	123	750
L15-4-lr	1.64	502	0.75	199	123	4	120	-	-	1.39	93	846
L15-5	1.66	516	0.62	267	209	3	147	542	106	1.72	65	695
N20-1-lr	1.40	311	1.93	157	42	7	118	-	-	5.30	122	190
N20-2	1.28	276	3.12	101	12	4	159	-	-	7.26	43	127
N20-3	1.38	299	1.98	125	15	5	138	[illegible]	[illegible]	4.42	54	225
N20-4	1.45	334	1.35	98	18	1	98	125	9	2.04	45	512
B15-1	1.24	164	1.25	92	16	1	97	102	1	1.03	155	866
B15-2	1.24	162	1.25	143	37	1	140	-	-	0.12	162	7753
B15-3	1.26	175	1.04	85	19	1	24	99	3	0.44	148	2050

(Wongwathanarat, Janka, Müller, ApJL 725 (2010) 106; A&A, to be submitted)

Neutron Star Recoil by "Gravitational Tug-Boat" Mechanism

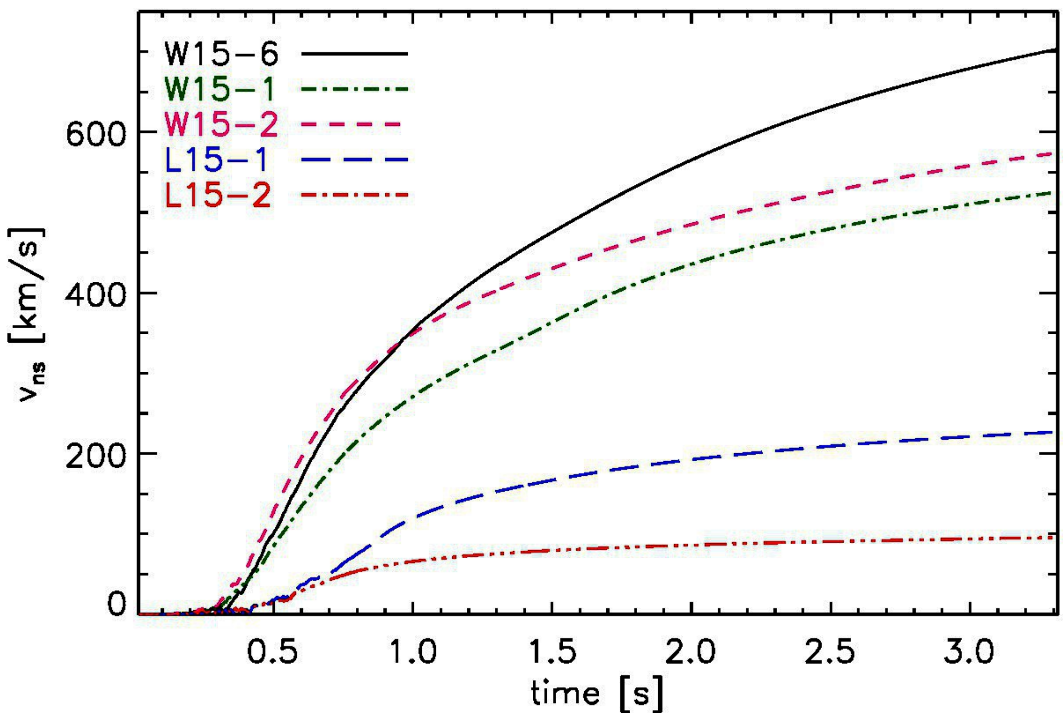

(Wongwathanarat, Janka, Müller, ApJL 725 (2010) 106; A&A, submitted, arXiv:1210.8148)

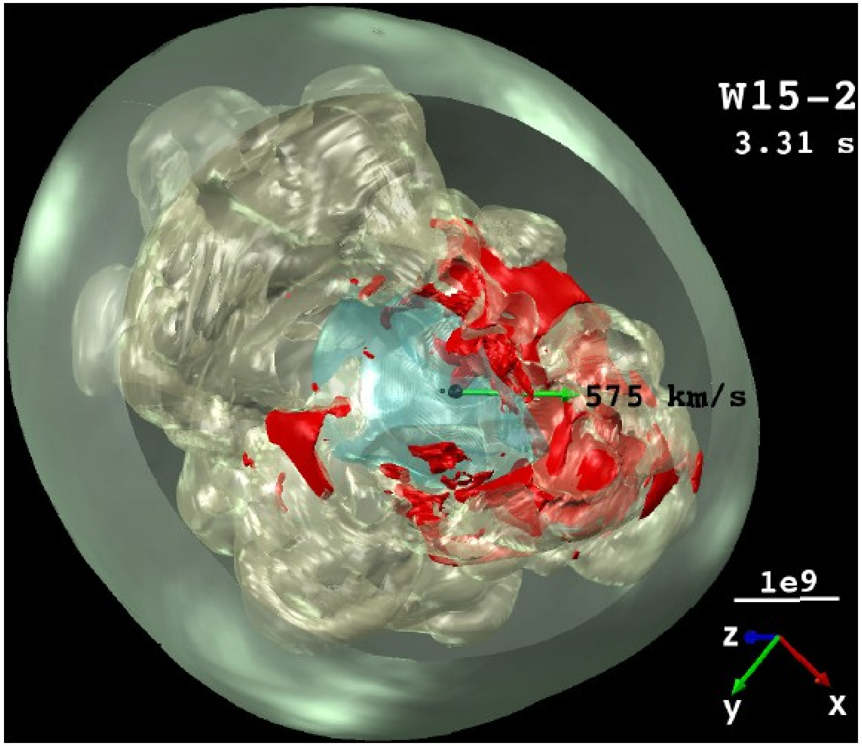

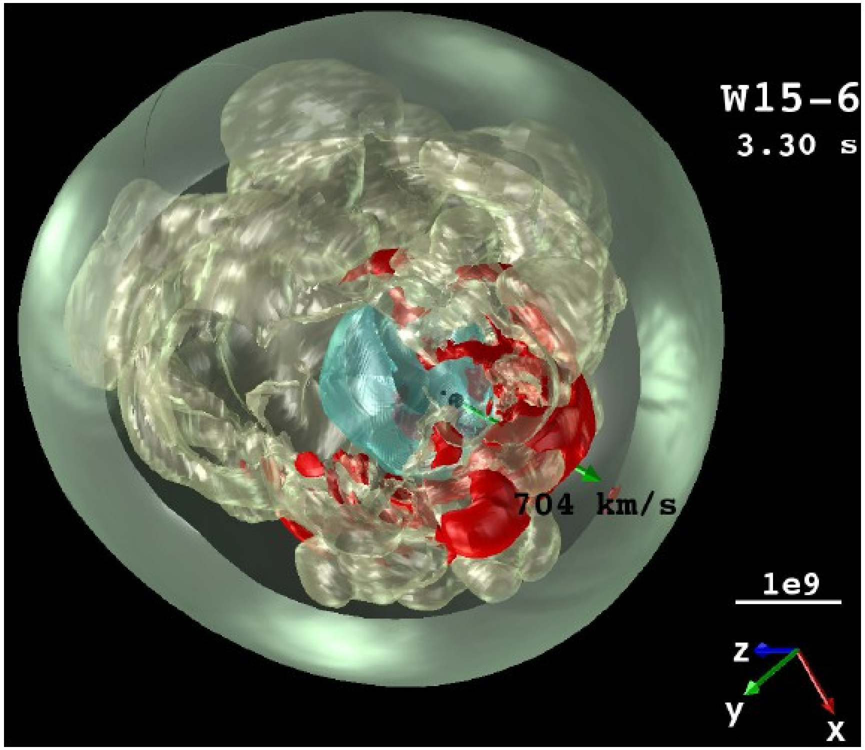

3D Explosions
and
Supernova Asymmetries

Mixing Instabilities in 3D SN Models

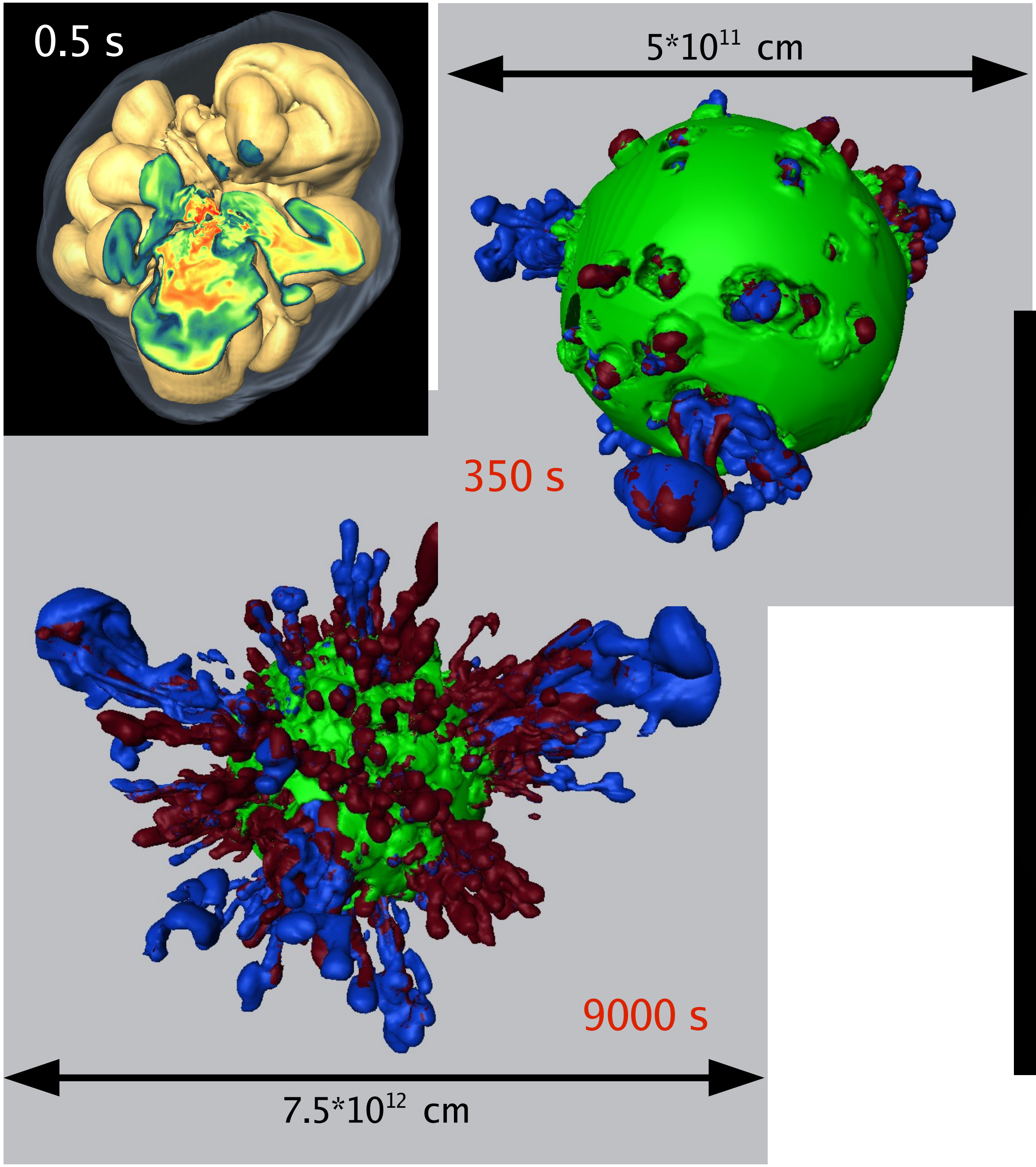

green: carbon
red: oxygen
blue: nickel

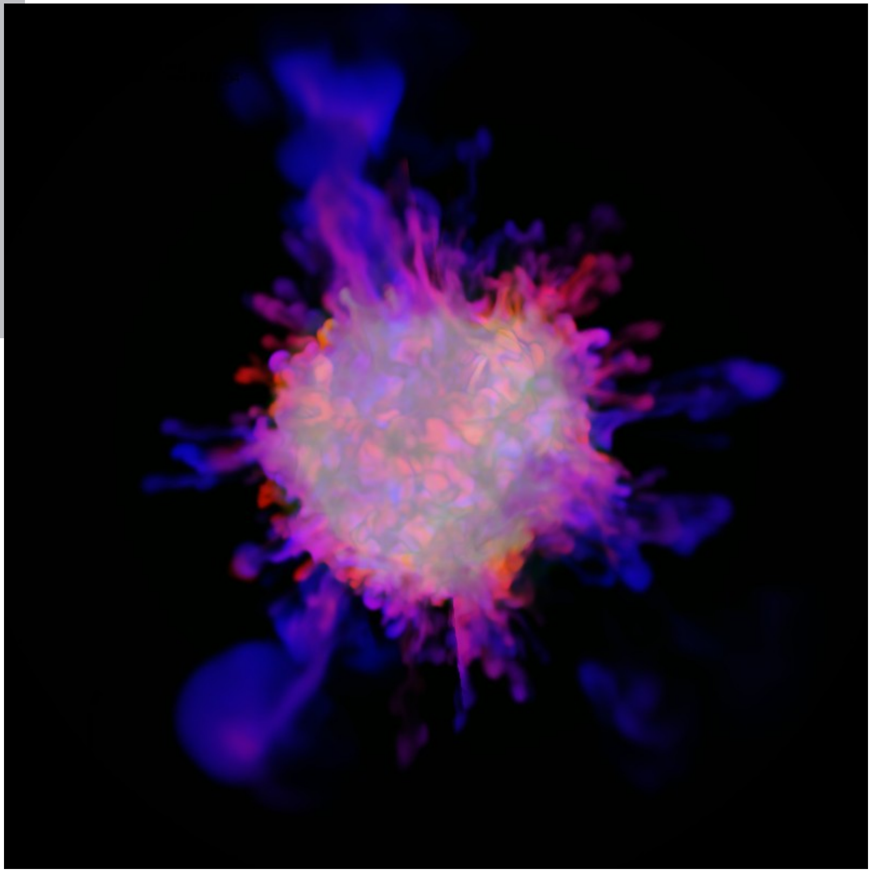

(Hammer, Janka, Müller, ApJ 2010)

Asymmetry of Supernova 1987A

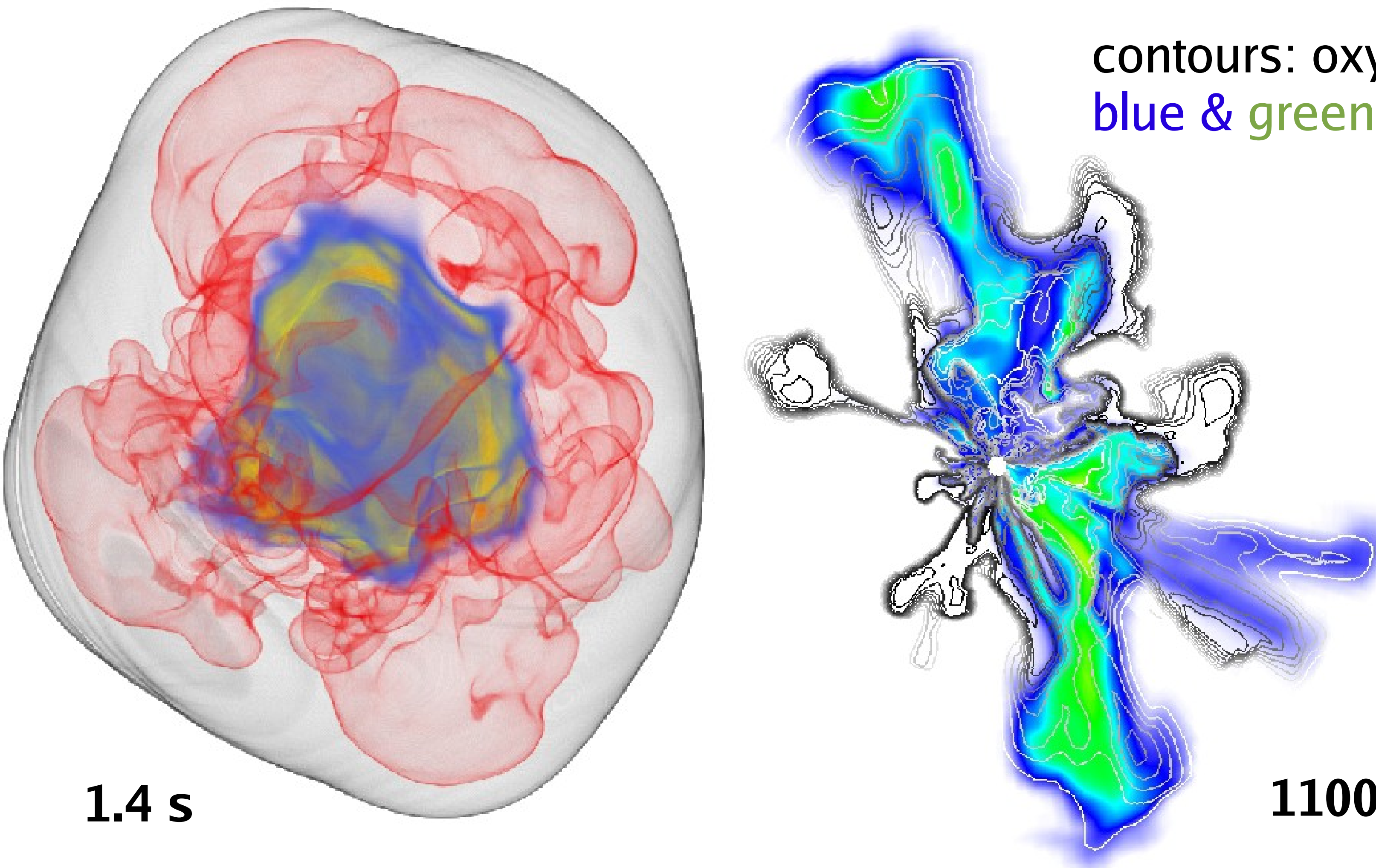

Relatively small convective asymmetries of early explosion can grow into large-scale asymmetry of the nickel and heavy-elements distributions!

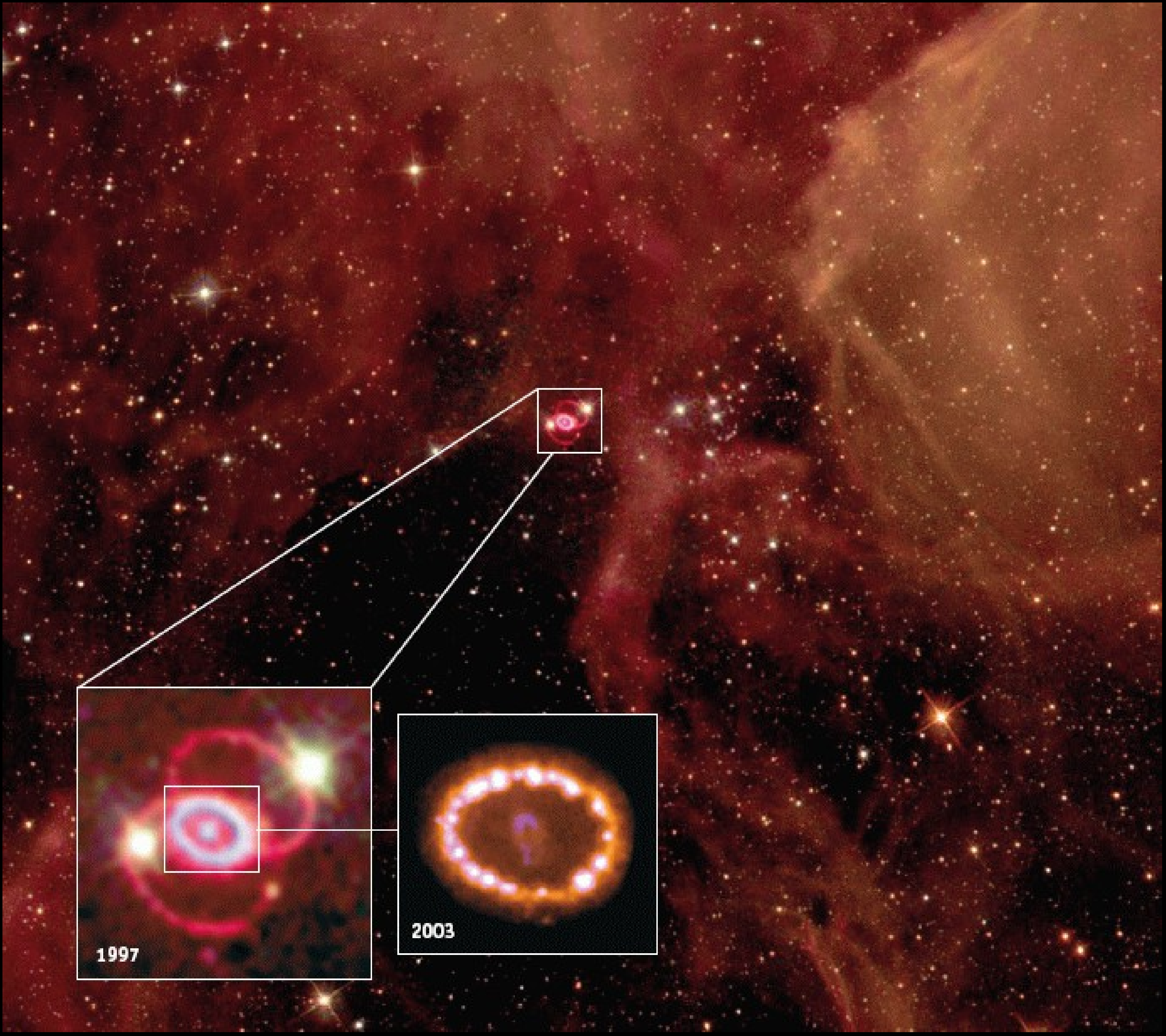

Supernova
1987A
as a
Teenager

Supernova 1987A

Observational consequences and indirect evidence of neutrino heating and hydrodynamic instabilities at the onset of stellar explosions:

- Neutron star kicks (Scheck et al. 2004, 2006; Wongwathanat et al. 2010, 2012)
- Asymmetric mass ejection & large-scale radial mixing
  (Kifonidis et al. 2005, Hammer er al. 2010)
- Characteristic neutrino-signal modulations
  (Marek et al. 2009; Müller et al. 2011, Lund et al. 2011, 2012)
- Gravitational-wave signals

But: Is neutrino heating strong enough to initiate the explosion?

Most sophisticated, self-consistent numerical simulations of the explosion mechanism in 2D and 3D are necessary!

Predictions of Signals from SN Core

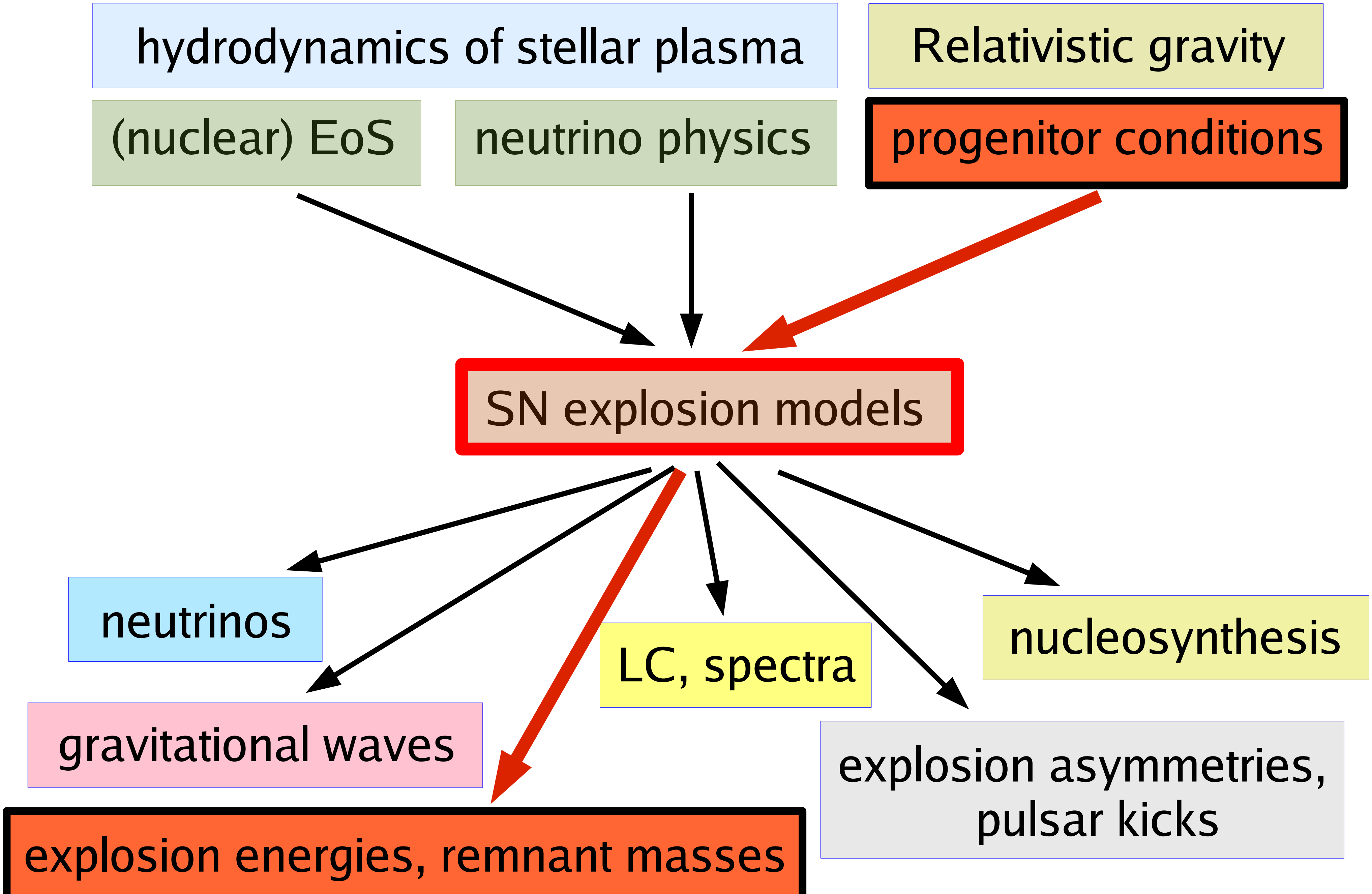

General-Relativistic 2D Supernova Models of the Garching Group

(Müller B., PhD Thesis (2009); Müller et al., ApJS, (2010))

GR hydrodynamics (CoCoNuT)

$$
\begin{aligned}
\frac{\partial \sqrt{\gamma}\rho W}{\partial t} + \frac{\partial \sqrt{-g}\rho W \hat{v}^i}{\partial x^i} &= 0, && (2.5)\\
\frac{\partial \sqrt{\gamma}\rho h W^2 v_j}{\partial t} + \frac{\partial \sqrt{-g}\left(\rho h W^2 v_j \hat{v}^i + \delta^i_j P\right)}{\partial x^i} &= \frac{1}{2}\sqrt{-g}T^{\mu\nu}\frac{\partial g_{\mu\nu}}{\partial x^j} + \left(\frac{\partial \sqrt{\gamma} S_j}{\partial t}\right)_C, && (2.6)\\
\frac{\partial \sqrt{\gamma}\tau}{\partial t} + \frac{\partial \sqrt{-g}\left(\tau \hat{v}^i + P v^i\right)}{\partial x^i} &= \alpha\sqrt{-g}\left(T^{\mu 0}\frac{\partial \ln \alpha}{\partial x^\mu} - T^{\mu\nu}\Gamma^0_{\mu\nu}\right) + \left(\frac{\partial \sqrt{\gamma}\tau}{\partial t}\right)_C. && (2.7)
\end{aligned}
$$

$$
\frac{\partial \sqrt{\gamma}\rho W Y_e}{\partial t} + \frac{\partial \sqrt{-g}\rho W Y_e \hat{v}^i}{\partial x^i} = \left(\frac{\partial \sqrt{\gamma}\rho W Y_e}{\partial t}\right)_C, \qquad (2.8)
$$

$$
\frac{\partial \sqrt{\gamma}\rho W X_k}{\partial t} + \frac{\partial \sqrt{-g}\rho W X_k \hat{v}^i}{\partial x^i} = 0. \qquad (2.9)
$$

CFC metric equations

$$
\begin{aligned}
\hat{\Delta}\Phi &= -2\pi\phi^5\left(E + \frac{K_{ij}K^{ij}}{16\pi}\right), && (2.10)\\
\hat{\Delta}(\alpha\Phi) &= 2\pi\alpha\phi^5\left(E + 2S + \frac{7K_{ij}K^{ij}}{16\pi}\right), && (2.11)\\
\hat{\Delta}\beta^i &= 16\pi\alpha\phi^4 S^i + 2\phi^{10}K^{ij}\hat{\nabla}_j\left(\frac{\alpha}{\Phi^6}\right) - \frac{1}{3}\hat{\nabla}^i\hat{\nabla}_j\beta^j, && (2.12)
\end{aligned}
$$

$$
\begin{aligned}
&\frac{\partial W\left(\hat{J} + v_r\hat{H}\right)}{\partial t} + \frac{\partial}{\partial r}\left[\left(W\frac{\alpha}{\phi^2} - \beta_r v_r\right)\hat{H} + \left(W v_r\frac{\alpha}{\phi^2} - \beta_r\right)\hat{J}\right] - \qquad (2.28)\\
&\quad \frac{\partial}{\partial \varepsilon}\left\{W\varepsilon\hat{J}\left[\frac{1}{r}\left(\beta_r - \frac{\alpha v_r}{\phi^2}\right) + 2\left(\beta_r - \frac{\alpha v_r}{\phi^2}\right)\frac{\partial \ln\phi}{\partial r} - 2\frac{\partial \ln\phi}{\partial t}\right] + \right.\\
&\quad W\varepsilon\hat{H}\left[v_r\left(\frac{\partial \beta_r\phi^2}{\partial r} - 2\frac{\partial \ln\phi}{\partial t}\right) - \frac{\alpha}{\phi^2}\frac{\partial \ln\alpha W}{\partial r} + \alpha W^2\left(\beta_r\frac{\partial v_r}{\partial r} - \frac{\partial v_r}{\partial t}\right)\right] - \\
&\quad \left.\varepsilon\hat{K}\left[\frac{\beta_r W}{r} - \frac{\partial \beta_r W}{\partial r} + W v_r r\frac{\partial}{\partial r}\left(\frac{\alpha}{r\phi^2}\right) + W^3\left(\frac{\alpha}{\phi^2}\frac{\partial v_r}{\partial r} + v_r\frac{\partial v_r}{\partial t}\right)\right]\right\} - \\
&\quad W\hat{J}\left[\frac{1}{r}\left(\beta_r - \frac{\alpha v_r}{\phi^2}\right) + 2\left(\beta_r - \frac{\alpha v_r}{\phi^2}\right)\frac{\partial \ln\phi}{\partial r} - 2\frac{\partial \ln\phi}{\partial t}\right] - \\
&\quad W\hat{H}\left[v_r\left(\frac{\partial \beta_r\phi^2}{\partial r} - 2\frac{\partial \ln\phi}{\partial t}\right) - \frac{\alpha}{\phi^2}\frac{\partial \ln\alpha W}{\partial r} + \alpha W^2\left(\beta_r\frac{\partial v_r}{\partial r} - \frac{\partial v_r}{\partial t}\right)\right] + \\
&\quad \hat{K}\left[\frac{\beta_r W}{r} - \frac{\partial \beta_r W}{\partial r} + W v_r r\frac{\partial}{\partial r}\left(\frac{\alpha}{r\phi^2}\right) + W^3\left(\frac{\alpha}{\phi^2}\frac{\partial v_r}{\partial r} + v_r\frac{\partial v_r}{\partial t}\right)\right] = \alpha\hat{C}^{(0)},
\end{aligned}
$$

Neutrino transport (VERTEX)

$$
\begin{aligned}
&\frac{\partial W\left(\hat{H} + v_r\hat{K}\right)}{\partial t} + \frac{\partial}{\partial r}\left[\left(W\frac{\alpha}{\phi^2} - \beta_r v_r\right)\hat{K} + \left(W v_r\frac{\alpha}{\phi^2} - \beta_r\right)\hat{H}\right] - \qquad (2.29)\\
&\quad \frac{\partial}{\partial \varepsilon}\left\{W\varepsilon\hat{H}\left[\frac{1}{r}\left(\beta_r - \frac{\alpha v_r}{\phi^2}\right) + 2\left(\beta_r - \frac{\alpha v_r}{\phi^2}\right)\frac{\partial \ln\phi}{\partial r} - 2\frac{\partial \ln\phi}{\partial t}\right] + \right.\\
&\quad W\varepsilon\hat{K}\left[v_r\left(\frac{\partial \beta_r\phi^2}{\partial r} - 2\frac{\partial \ln\phi}{\partial t}\right) - \frac{\alpha}{\phi^2}\frac{\partial \ln\alpha W}{\partial r} + \alpha W^2\left(\beta_r\frac{\partial v_r}{\partial r} - \frac{\partial v_r}{\partial t}\right)\right] - \\
&\quad \left.\varepsilon\hat{L}\left[\frac{\beta_r W}{r} - \frac{\partial \beta_r W}{\partial r} + W v_r r\frac{\partial}{\partial r}\left(\frac{\alpha}{r\phi^2}\right) + W^3\left(\frac{\alpha}{\phi^2}\frac{\partial v_r}{\partial r} + v_r\frac{\partial v_r}{\partial t}\right)\right]\right\} + \\
&\quad \left(\hat{J} - \hat{K}\right)\left[v_r\left(\frac{\beta_r}{r} - \frac{\partial \beta_r}{\partial r}\right) + \frac{\partial}{\partial r}\left(\frac{W\alpha}{\phi^2}\right) - \frac{W\alpha}{r\phi^2} + W^3\left(\frac{\partial v_r}{\partial t} - \beta_r\frac{\partial v_r}{\partial r}\right)\right] + \\
&\quad \left(\hat{H} - \hat{L}\right)\left[\frac{W^3\alpha}{\phi^2}\frac{\partial v_r}{\partial r} + \frac{\beta W}{r} - \frac{\partial \beta W}{\partial r} - W v_r r\frac{\partial}{\partial r}\left(\frac{\alpha}{r\phi^2}\right) + \frac{\partial W}{\partial t}\right] - \\
&\quad W\hat{H}\left[\frac{1}{r}\left(\beta_r - \frac{\alpha v_r}{\phi^2}\right) + 2\left(\beta_r - \frac{\alpha v_r}{\phi^2}\right)\frac{\partial \ln\phi}{\partial r} - 2\frac{\partial \ln\phi}{\partial t}\right] - \\
&\quad W\hat{K}\left[v_r\left(\frac{\partial \beta_r\phi^2}{\partial r} - 2\frac{\partial \ln\phi}{\partial t}\right) - \frac{\alpha}{\phi^2}\frac{\partial \ln\alpha W}{\partial r} + \alpha W^2\left(\beta_r\frac{\partial v_r}{\partial r} - \frac{\partial v_r}{\partial t}\right)\right] + \\
&\quad \hat{L}\left[\frac{\beta_r W}{r} - \frac{\partial \beta_r W}{\partial r} + W v_r r\frac{\partial}{\partial r}\left(\frac{\alpha}{r\phi^2}\right) + W^3\left(\frac{\alpha}{\phi^2}\frac{\partial v_r}{\partial r} + v_r\frac{\partial v_r}{\partial t}\right)\right] = \alpha\hat{C}^{(1)}.
\end{aligned}
$$

Neutrino Reactions in Supernovae

Beta processes:	• $e^- + p \rightleftharpoons n + \nu_e$ • $e^+ + n \rightleftharpoons p + \bar{\nu}_e$ • $e^- + A \rightleftharpoons \nu_e + A^*$
Neutrino scattering:	• $\nu + n, p \rightleftharpoons \nu + n, p$ • $\nu + A \rightleftharpoons \nu + A$ • $\nu + e^\pm \rightleftharpoons \nu + e^\pm$
Thermal pair processes:	• $N + N \rightleftharpoons N + N + \nu + \bar{\nu}$ • $e^+ + e^- \rightleftharpoons \nu + \bar{\nu}$
Neutrino-neutrino reactions:	• $\nu_x + \nu_e, \bar{\nu}_e \rightleftharpoons \nu_x + \nu_e, \bar{\nu}_e$ $(\nu_x = \nu_\mu, \bar{\nu}_\mu, \nu_\tau, \text{or } \bar{\nu}_\tau)$ • $\nu_e + \bar{\nu}_e \rightleftharpoons \nu_{\mu,\tau} + \bar{\nu}_{\mu,\tau}$

The Curse and Challenge of the Dimensions

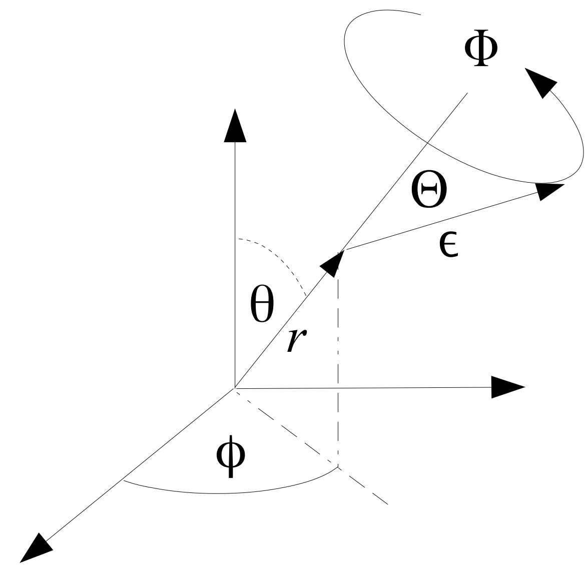

Boltzmann equation determines neutrino distribution function in 6D phase space and time

$$f\left(r,\theta,\phi,\Theta,\Phi,\epsilon,t\right)$$

Integration over 3D momentum space yields source terms for hydrodynamics

$$Q\left(r,\theta,\phi,t\right),\dot{Y}_e\left(r,\theta,\phi,t\right)$$

Solution approach	**Required resources**
• **3D** hydro + **6D** direct discretization of Boltzmann Eq. (code development by Sumiyoshi & Yamada '12)	• ≥ 10–100 PFlops/s (sustained!)
• **3D** hydro + two-moment closure of Boltzmann Eq. (next feasible step to full 3D; cf. Kuroda et al. 2012)	• ≥ 1–10 Pflops/s, TBytes
• **3D** hydro + "**ray-by-ray-plus**" variable Eddington factor method (method used at MPA/Garching)	• ≥ 0.1–1 PFlops/s, Tbytes
• **2D** hydro + "**ray-by-ray-plus**" variable Eddington factor method (method used at MPA/Garching)	• ≥ 0.1–1 Tflops/s, < 1 TByte

"Ray-by-Ray" Approximation for Neutrino Transport in 2D and 3D Geometry

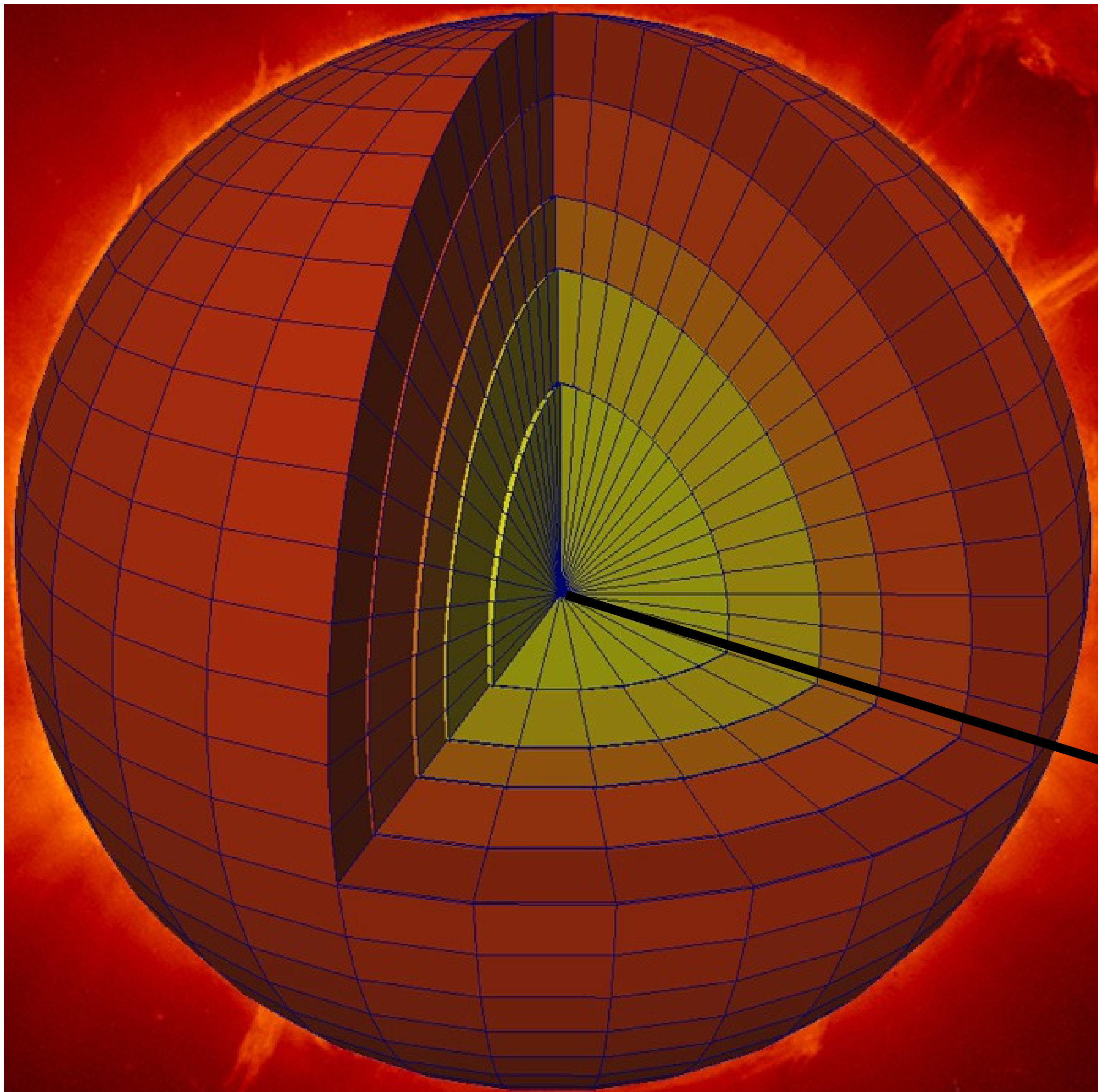

Solve large number of spherical transport problems on radial “rays” associated with angular zones of polar coordinate grid

Suggests efficient parallization over the “rays”

Performance and Portability of our Supernova Code *Prometheus-Vertex*

- Code employs hybrid MPI/OpenMP programming model (collaborative development with **Katharina Benkert, HLRS**).
- Code has been ported to different computer platforms by **Andreas Marek, High Level Application Support, Rechenzentrum Garching (RZG).**
- Code shows excellent parallel efficiency, which will be fully exploited in 3D.

Strong Scaling

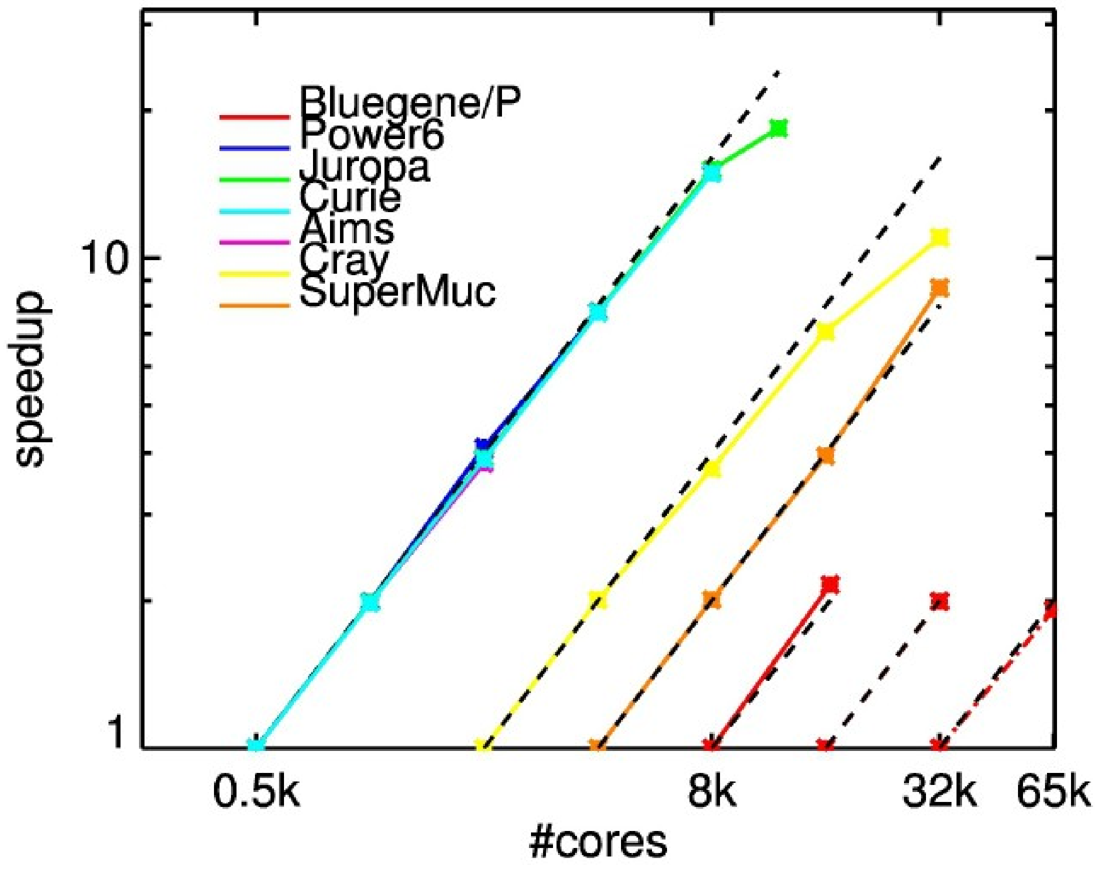

Andreas Marek, RZG (2012)

Computing Requirements for 2D & 3D Supernova Modeling

Time-dependent simulations: t ~ 1 second, ~ 10^6 time steps!

CPU-time requirements for one model run:

- **In 2D with 600 radial zones, 1 degree lateral resolution:**

  ~ $3*10^{18}$ Flops, need ~10^6 processor-core hours.

- **In 3D with 600 radial zones, 1.5 degrees angular resolution:**

  ~ $3*10^{20}$ Flops, need ~10^8 processor-core hours.

Explosion Mechanism: Most Sophisticated Current Models

Relativistic 2D CCSN Explosion Models

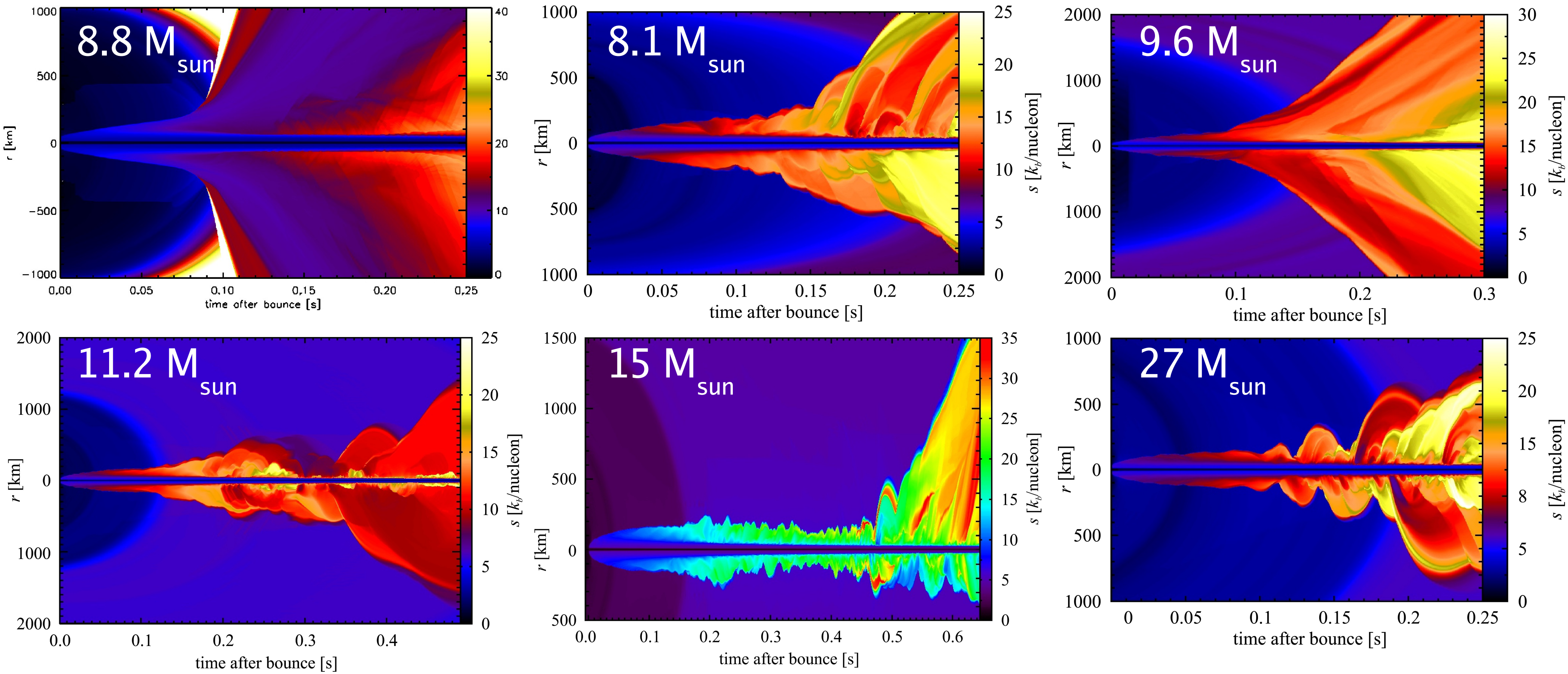

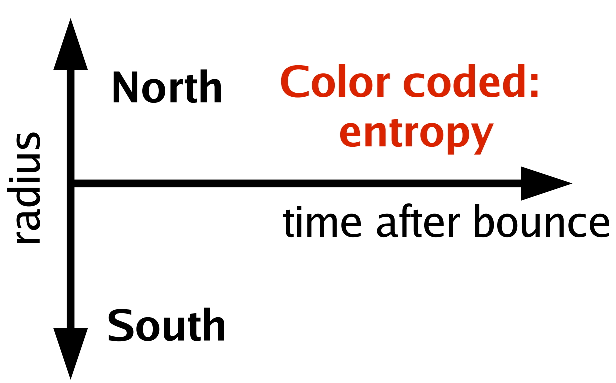

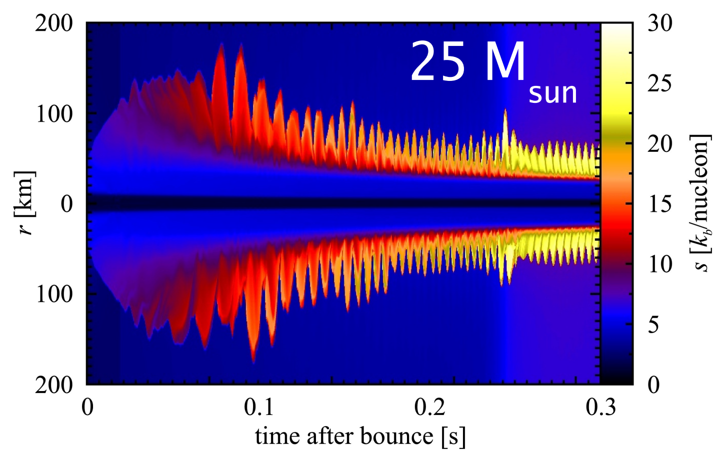

Bernhard Müller, THJ, et al. (ApJ 756, ApJ 761, arXiv:1210.6984

Basic confirmation of previous explosion models for 11.2 and 15 M_{sun} stars by Marek & THJ (2009)

Relativistic 2D CCSN Explosion Models

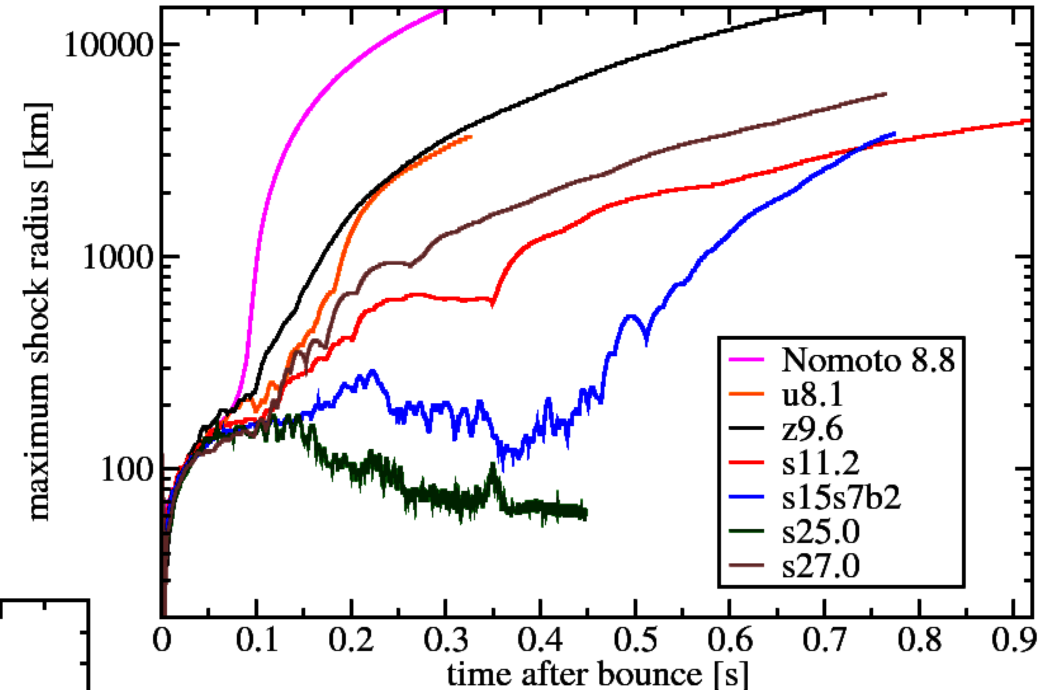

Maximum shock radius

"Diagnostic energy" of explosion

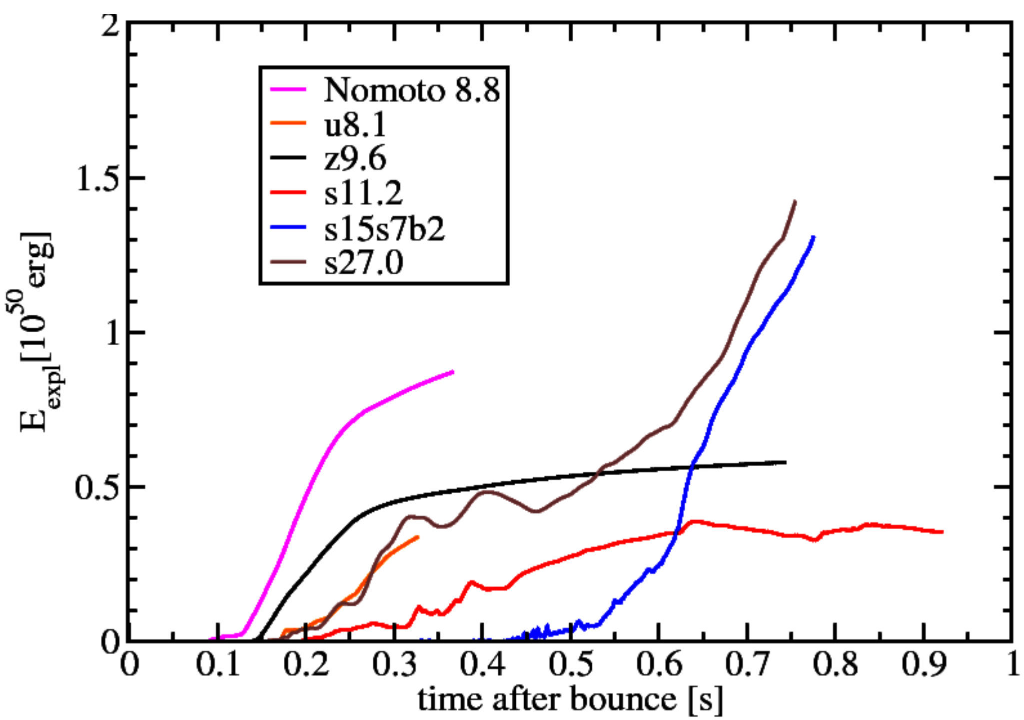

Support for 2D CCSN Explosion Models

2D explosions for 13 M_{sun} progenitor of Nomoto & Hashimoto (1988)

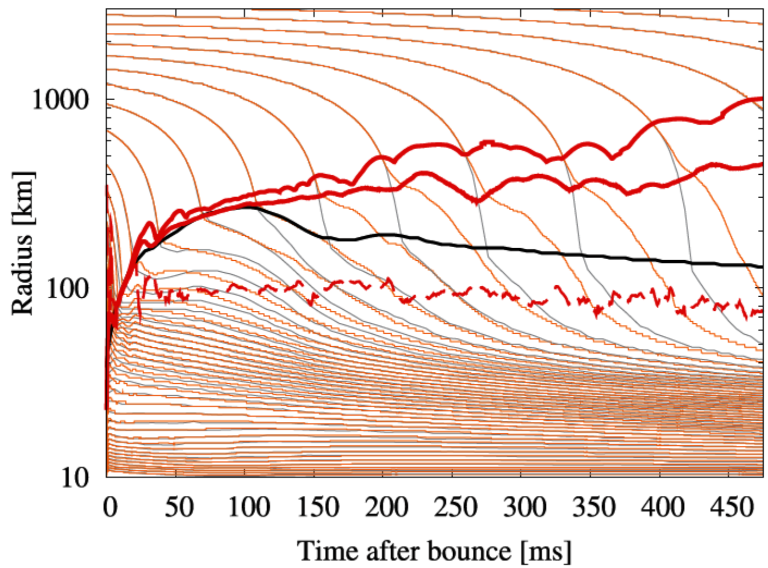

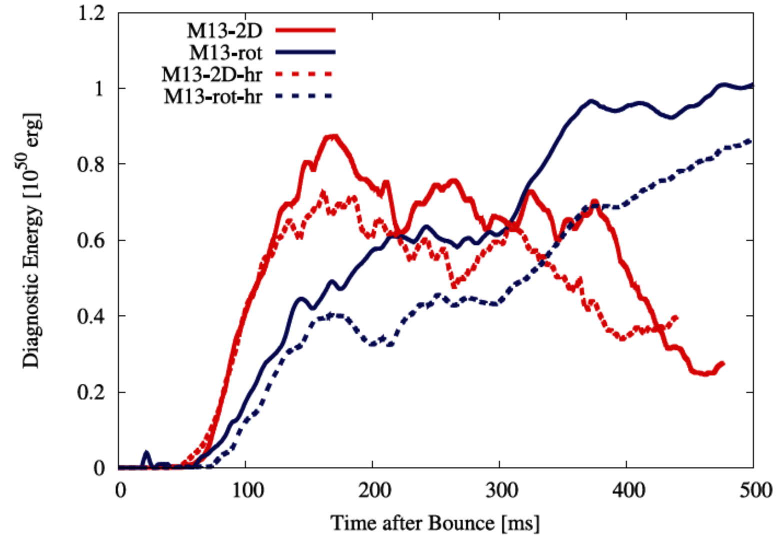

Suwa et al. (PASJ 62 (2010) L49

2D explosions for 11.2 and 15 M_{sun} progenitors of Woosley et al. (2002, 1995)

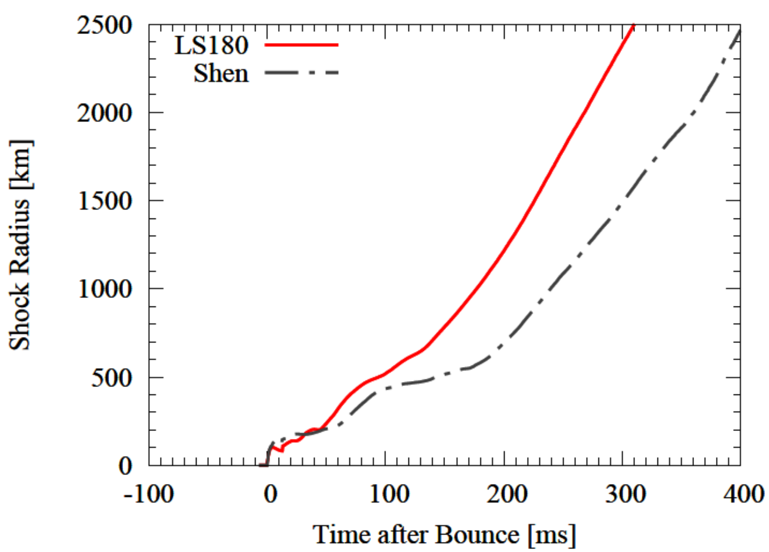

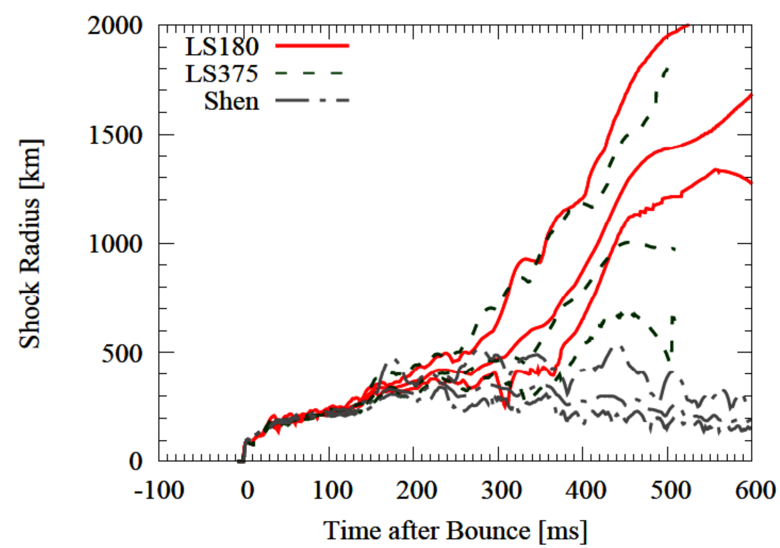

Suwa et al., arXiv:1206.6101

Support for 2D CCSN Explosion Models

2D explosions for 12, 15, 20, 25 M_{sun} progenitors of Woosley & Heger (2007)

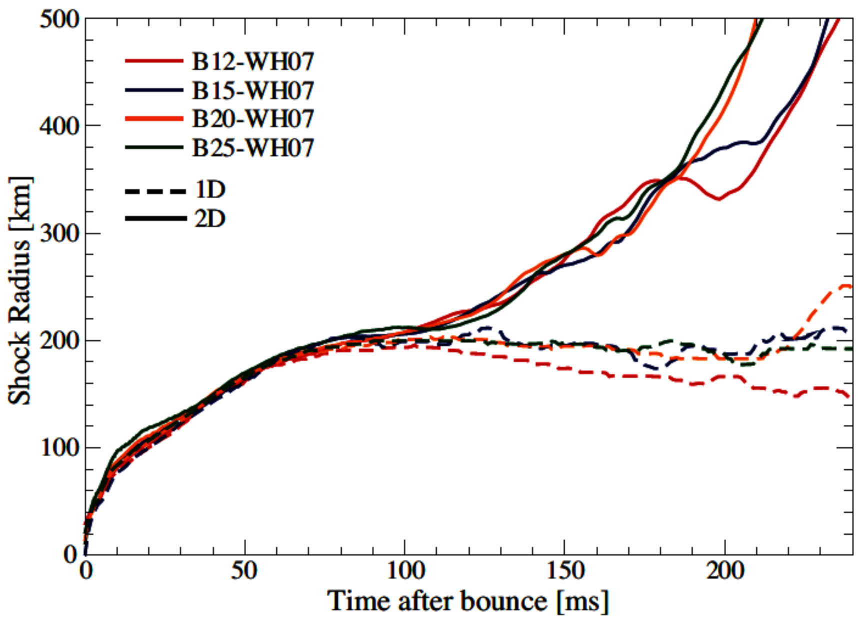

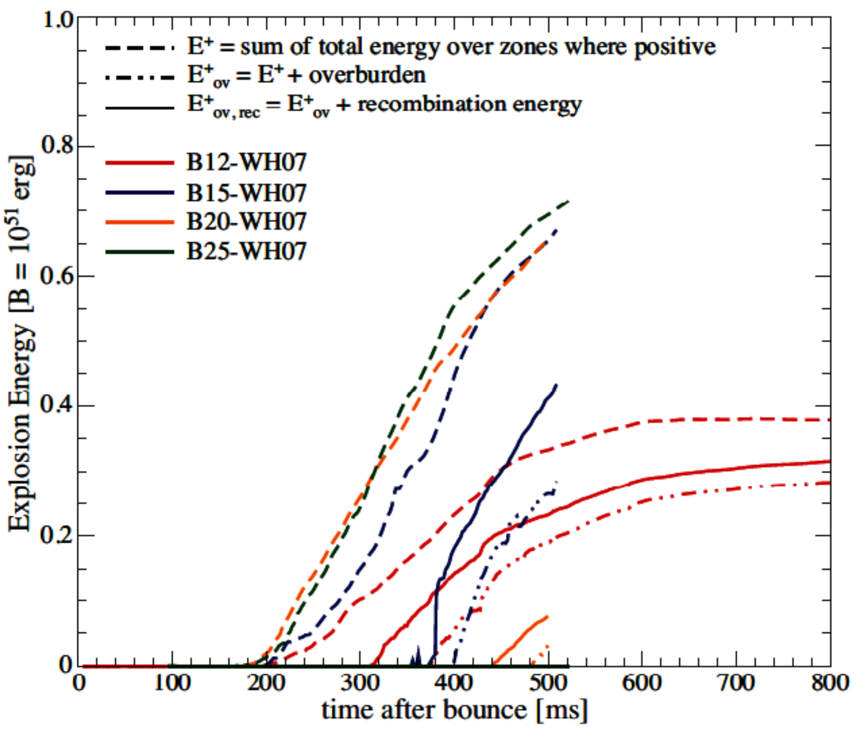

Bruenn et al., arXiv:1212.1747

2D SN Explosion Models

- Basic confirmation of the neutrino-driven mechanism
- Confirm reduction of the critical neutrino luminosity that enables an explosion in self-consistent 2D treatments compared to 1D

However, many aspects are different:

- Different codes, EoS treatment, neutrino transport and reactions
- Different progenitor sets
- Different explosion energies

Comparisons are urgently needed!

One more caveat:

2D explosions depend on the employed neutron-star equation of state

Neutron Star Equations of State

Neutron star EoS is crucial ingredient but incompletely known!

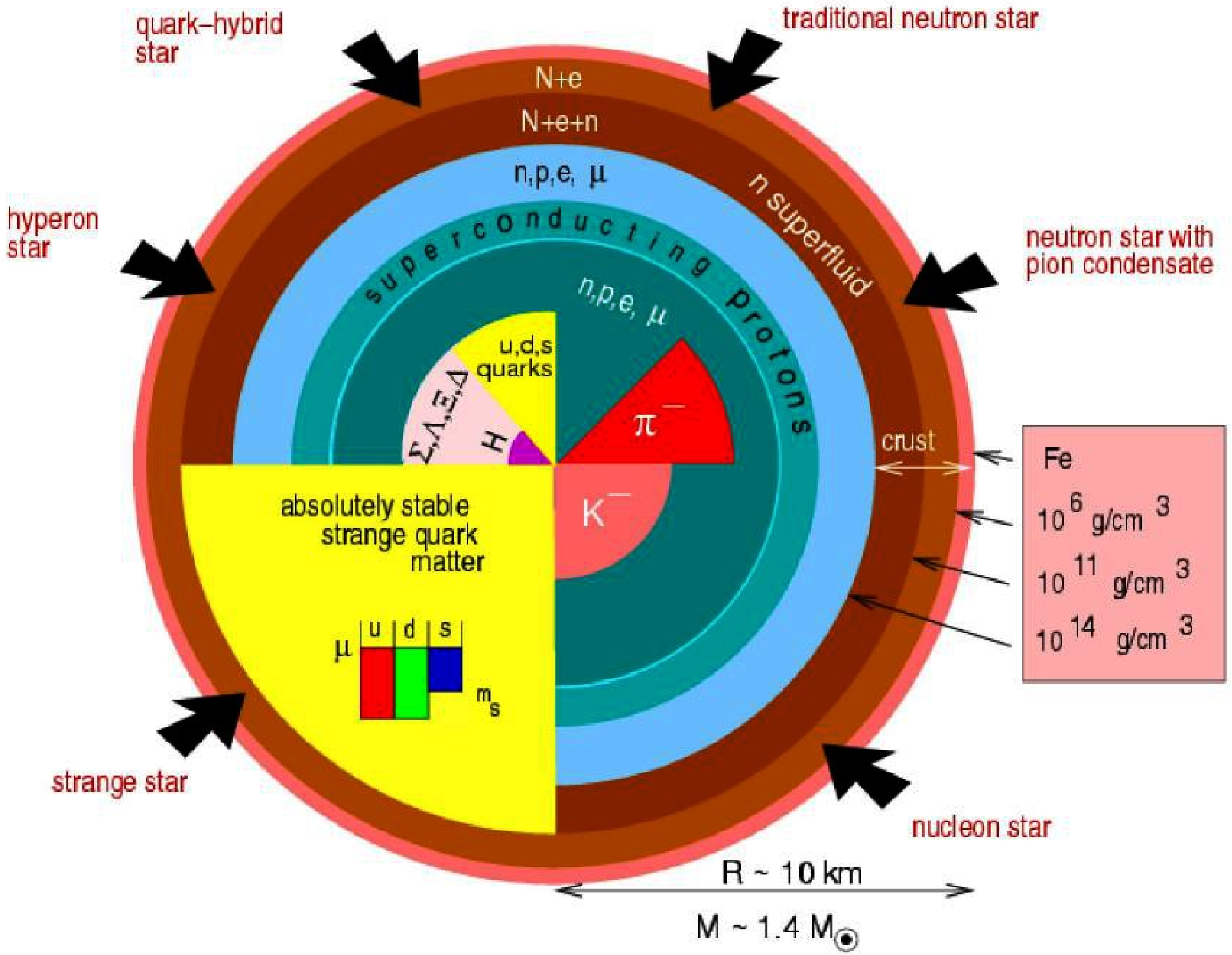

(Source: F. Weber)

Neutron Star Equations of State

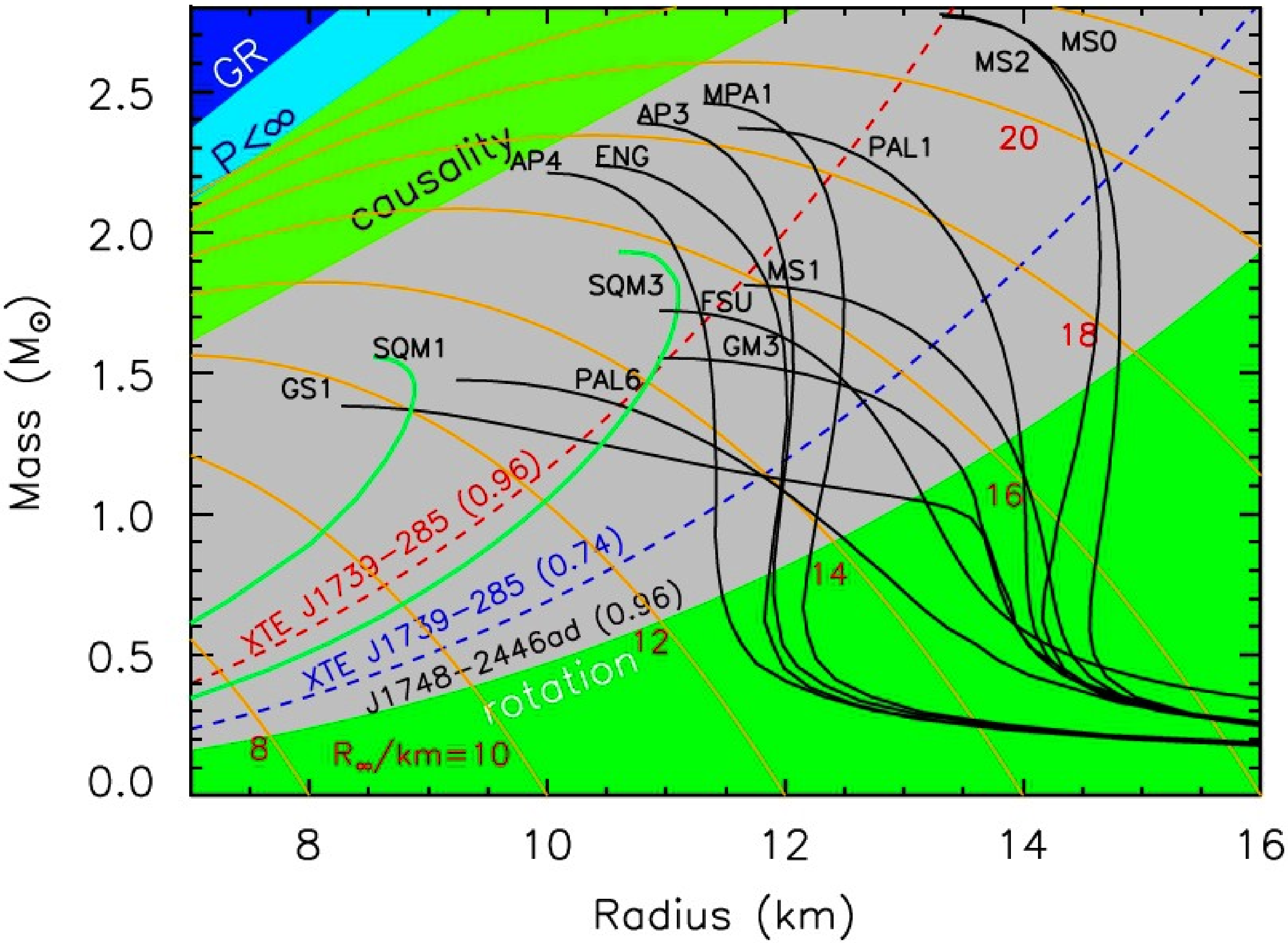

- Collapse and bounce show dependences on the EoS properties below and around nuclear saturation density ρ_0
- SN explosion and protoneutron star cooling are sensitive to the high-density EoS above ρ_0 through the compactness of the proto-neutron star
- Neutrino signal contains information about the nuclear EoS!

Lattimer & Prakash, Phys. Rep. 442 (2007)

2D Explosions of 11.2 M_{sun} star : Test of EoS Influence

- Simulations for 3 different nuclear EoSs:

  Lattimer & Swesty (L&S), Hillebrandt & Wolff (H&W), Shen et al.

- "Softer" (L&S) EoS and thus more compact PNS leads to earlier explosion.
- Reasons: more neutrino heating, more violent convective activity.

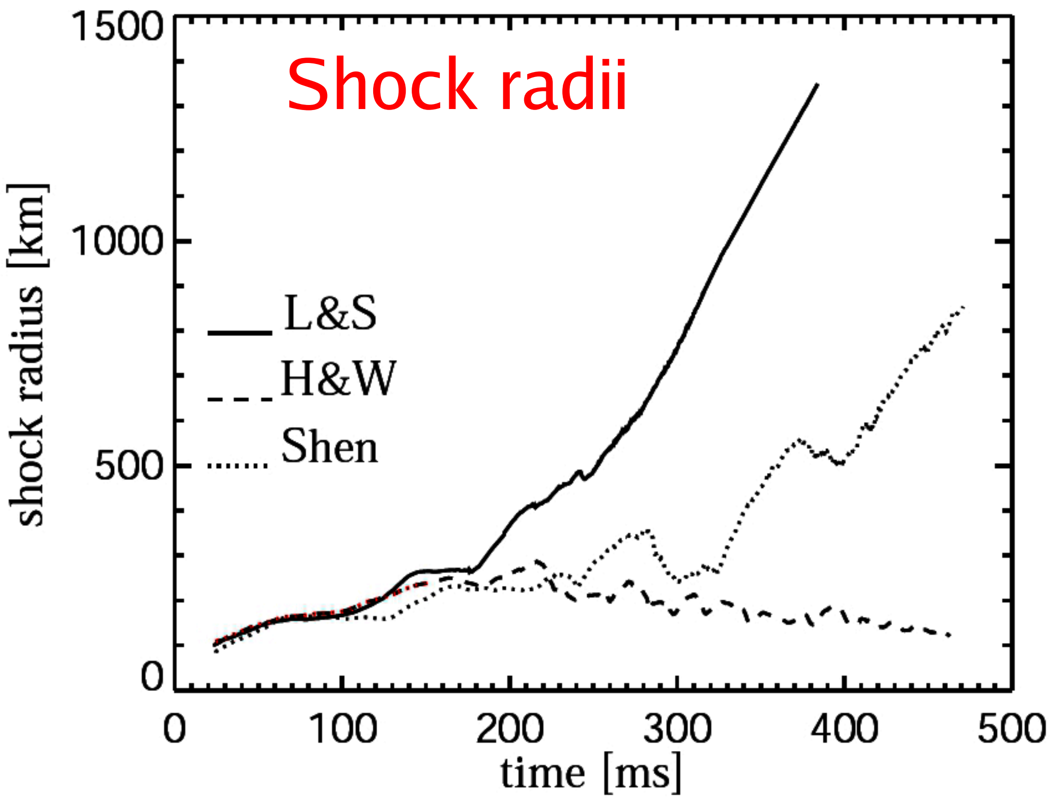

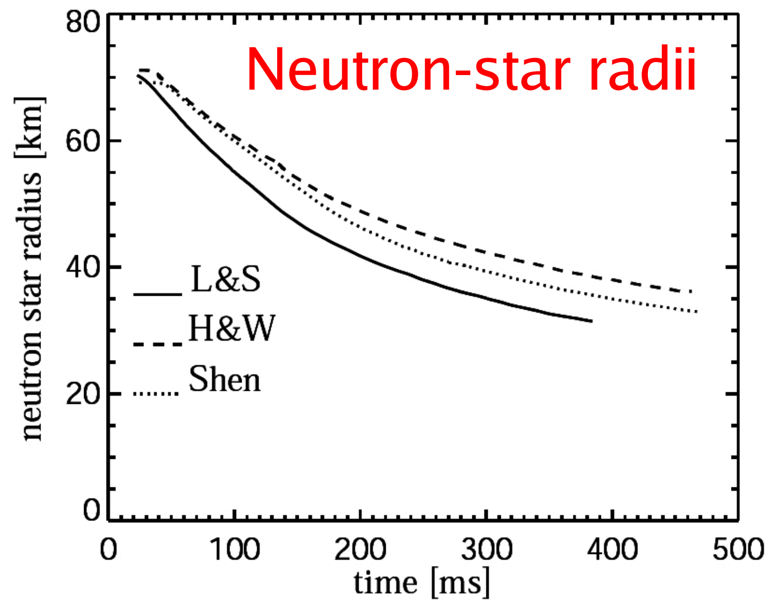

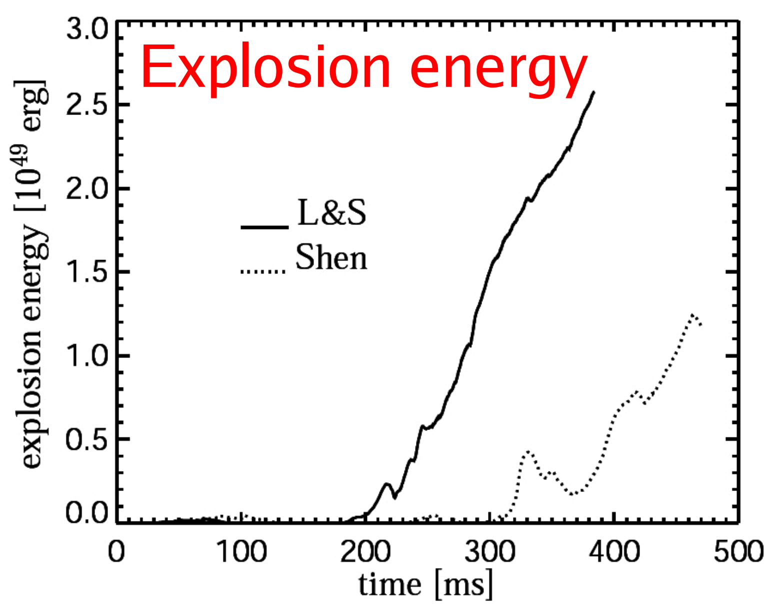

(Andreas Marek 2010, unpublished)

2D Explosions of 11.2 M_{sun} star : Test of EoS Influence

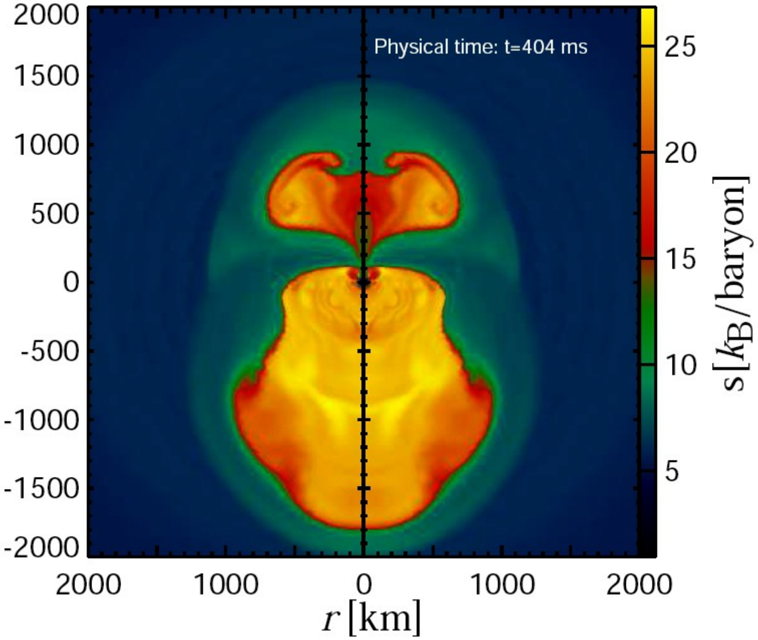

L&S EoS, t ~ 400 ms p.b.

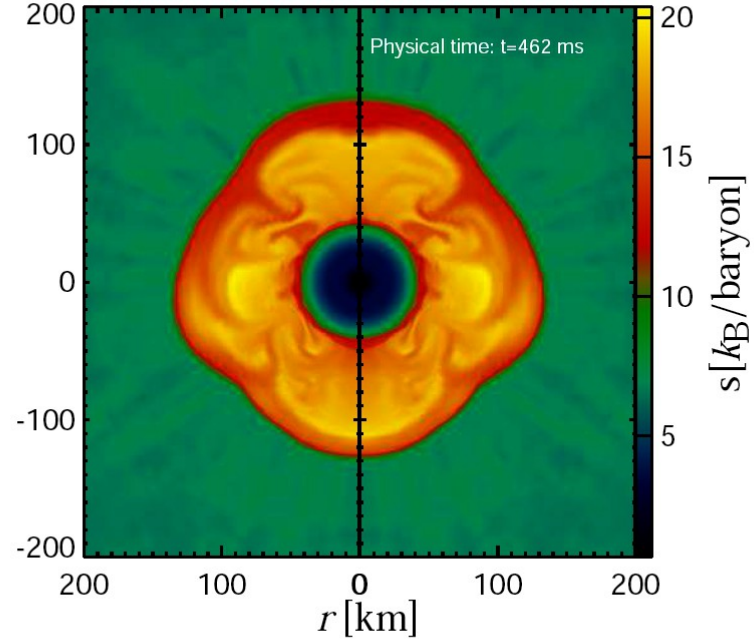

H&W EoS, t ~ 460 ms p.b.

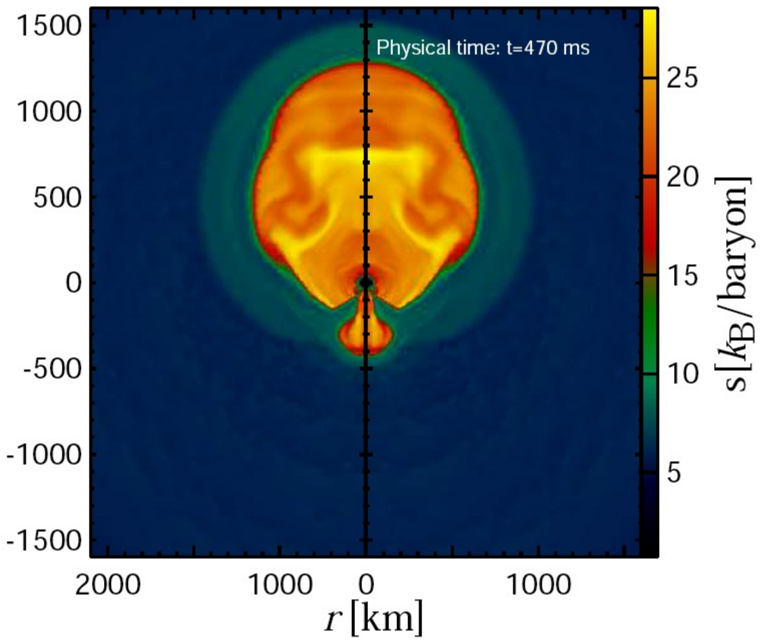

Shen EoS,
t ~ 470 ms p.b.

(Andreas Marek 2010,
unpublished)

Support for 2D CCSN Explosion Models

Suwa et al. (2012) also found that 2D explosions for 11.2 and 15 M_{sun} progenitors of Woosley et al. (2002, 1995) depend on the employed nuclear EoS.

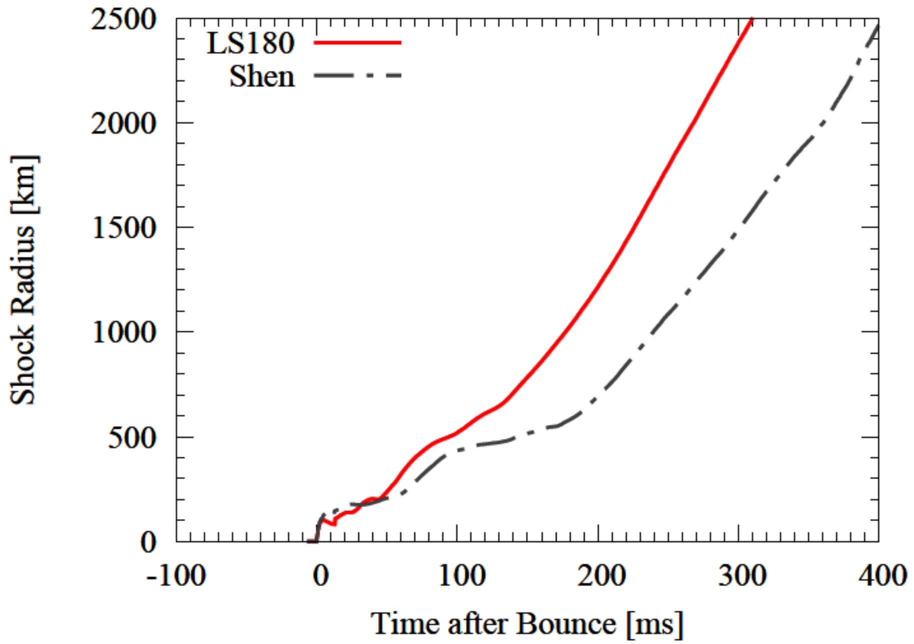

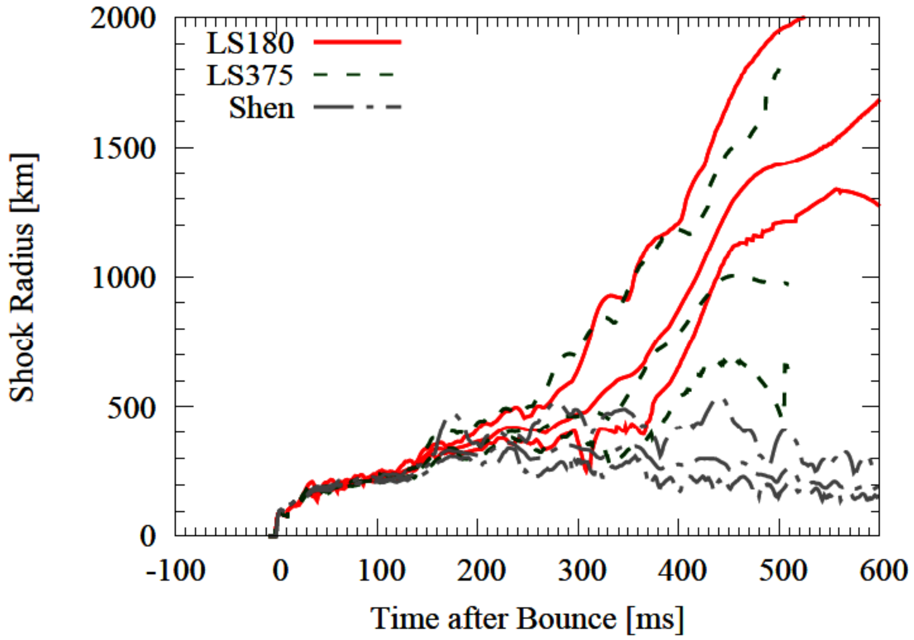

Suwa et al., arXiv:1206.6101

Der Optimist sagt: „Das Glas ist halb voll“
Der Pessimist sagt: „Das Glas ist halb leer“

[unbekannt]

Problems & Challenges

- 2D explosions seem to be "marginal", at least for some progenitor models and in some (the most?) sophisticated simulations.
- Nature is three dimensional, but 2D models impose the constraint of axisymmetry on the flow!
- Turbulent cascade in 3D transports energy from large to small scales, which is opposite to 2D.
- Is 3D turbulence more supportive to an explosion?
  Is the third dimension the key to the neutrino mechanism?
- 3D models are needed to confirm explosion mechanism suggested by 2D simulations!

3D vs. 2D Differences:

The Dimension Conundrum

2D-3D Differences in Parametric Explosion Models

- Nordhaus et al. (ApJ 720 (2010) 694) performed 2D & 3D simulations with simple neutrino- heating and cooling terms (no neutrino transport but lightbulb) and found 15–25% improvement in 3D for 15 M_{sun} progenitor star (ApJ 720 (2010) 694)

$$\mathcal{H} = 1.544 \times 10^{20} \left(\frac{L_{\nu_e}}{10^{52}\ \mathrm{erg\ s^{-1}}}\right)\left(\frac{T_{\nu_e}}{4\ \mathrm{MeV}}\right)^2 \times \left(\frac{100\ \mathrm{km}}{r}\right)^2 (Y_\mathrm{n} + Y_\mathrm{p}) e^{-\tau_{\nu_e}} \left[\frac{\mathrm{erg}}{\mathrm{g\ s}}\right]$$

$$\mathcal{C} = 1.399 \times 10^{20} \left(\frac{T}{2\ \mathrm{MeV}}\right)^6 (Y_\mathrm{n} + Y_\mathrm{p}) e^{-\tau_{\nu_e}} \left[\frac{\mathrm{erg}}{\mathrm{g\ s}}\right]$$

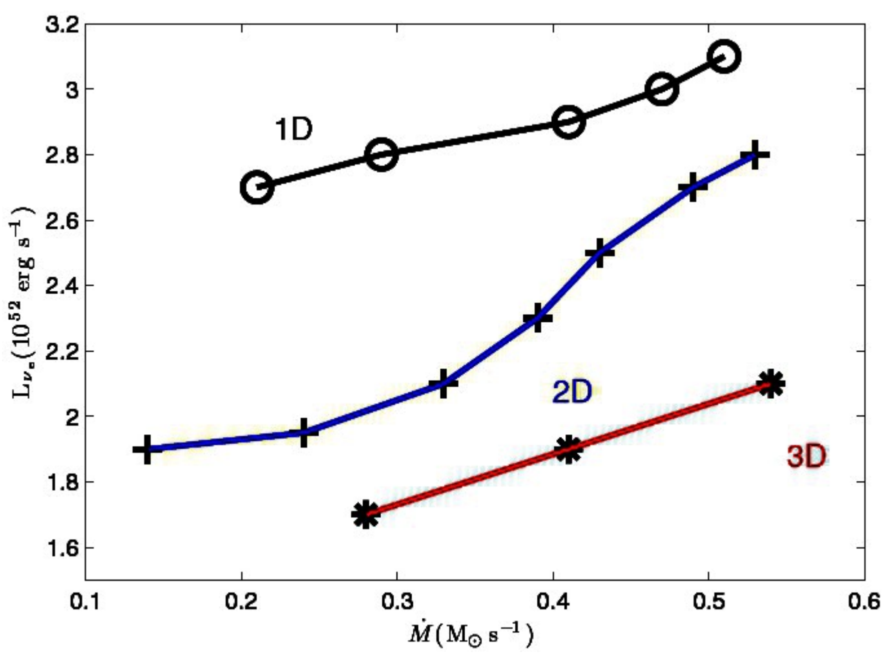

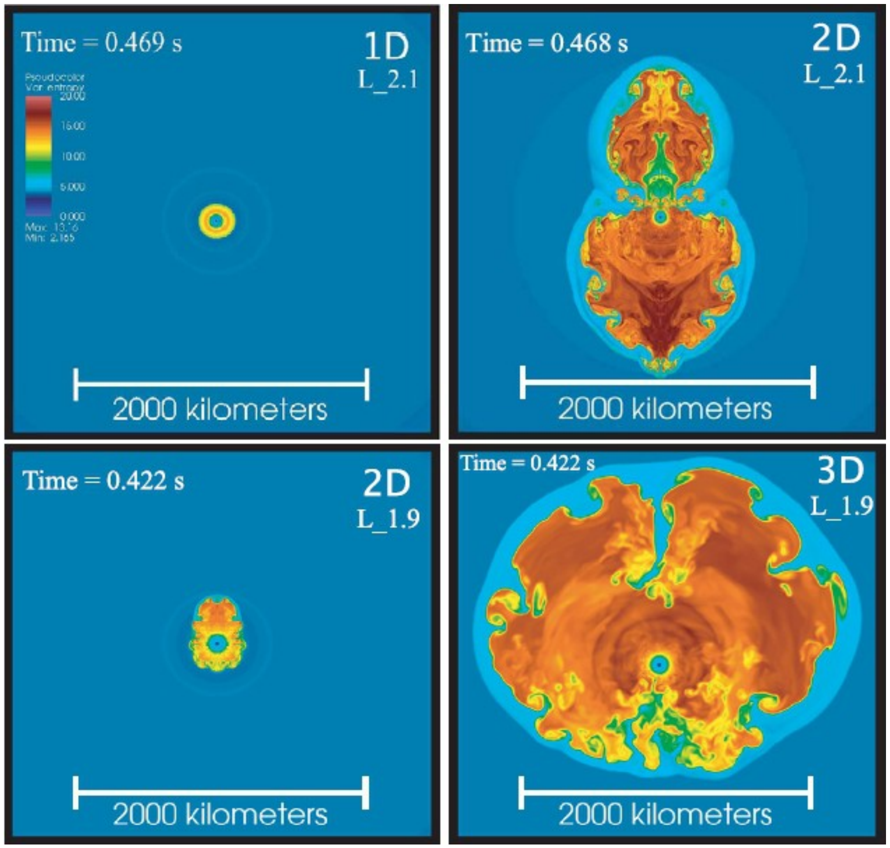

2D-3D Differences in Parametric Explosion Models

- F. Hanke (Diploma Thesis, MPA, 2010) in agreement with L. Scheck (PhD Thesis, MPA, 2007) could not confirm the findings by Nordhaus et al. (2010) ! 2D and 3D simulations for 11.2 M_{sun} and 15 M_{sun} progenitors are very similar but results depend on numerical grid resolution: 2D with higher resolution explodes easier, 3D shows opposite trend!

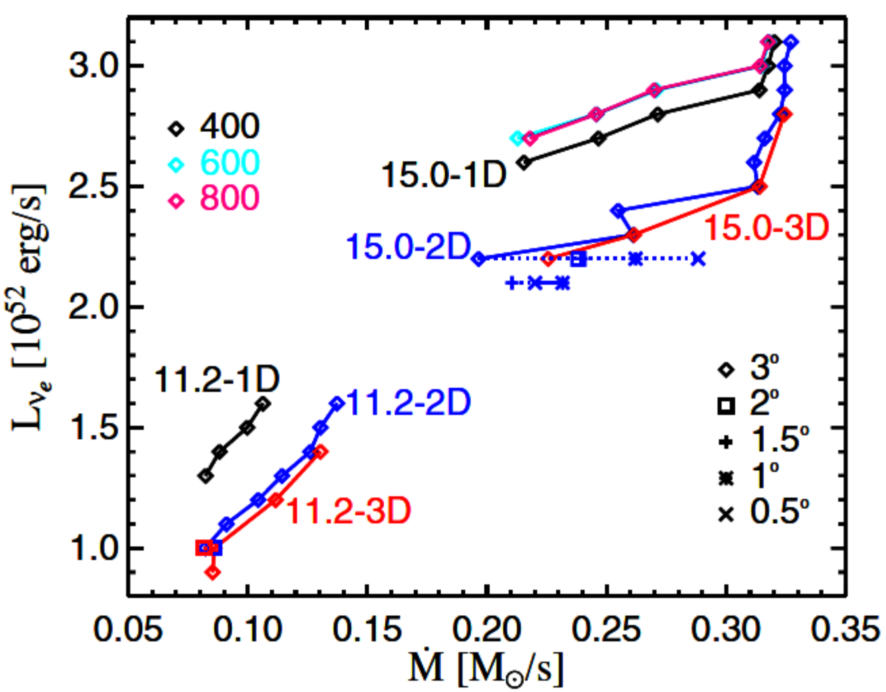

Hanke et al., ApJ 755 (2012) 138, arXiv:1108.4355

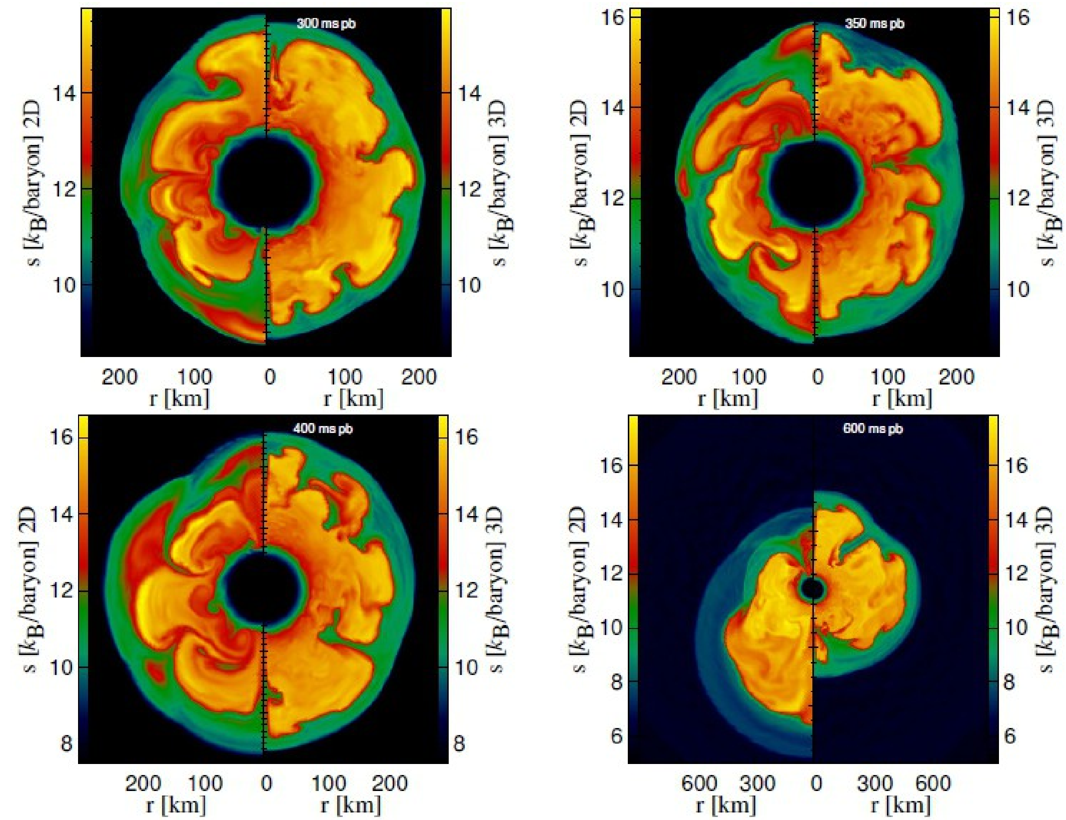

2D & 3D slices for 11.2 M_{sun} model, L = 1.0*10^{52} erg/s

2D-3D Differences in Parametric Explosion Models

- F. Hanke (Diploma Thesis, MPA, 2010) in agreement with L. Scheck (PhD Thesis, MPA, 2007) could not confirm the findings by Nordhaus et al. (2010) ! 2D and 3D simulations for 11.2 M_{sun} and 15 M_{sun} progenitors are very similar but results depend on numerical grid resolution: 2D with higher resolution explodes easier, 3D shows opposite trend!

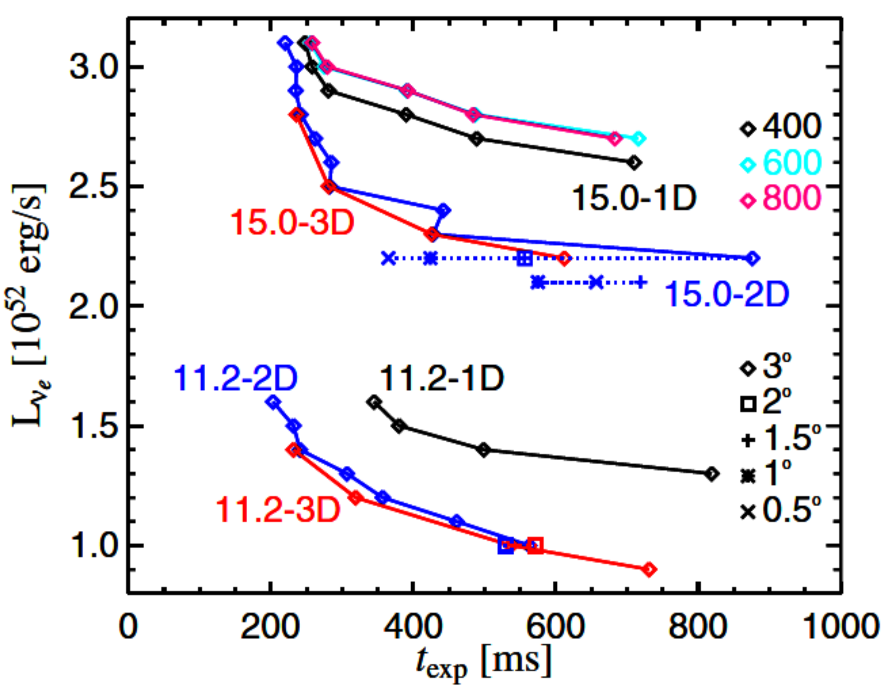

Hanke et al., ApJ 755 (2012) 138, arXiv:1108.4355

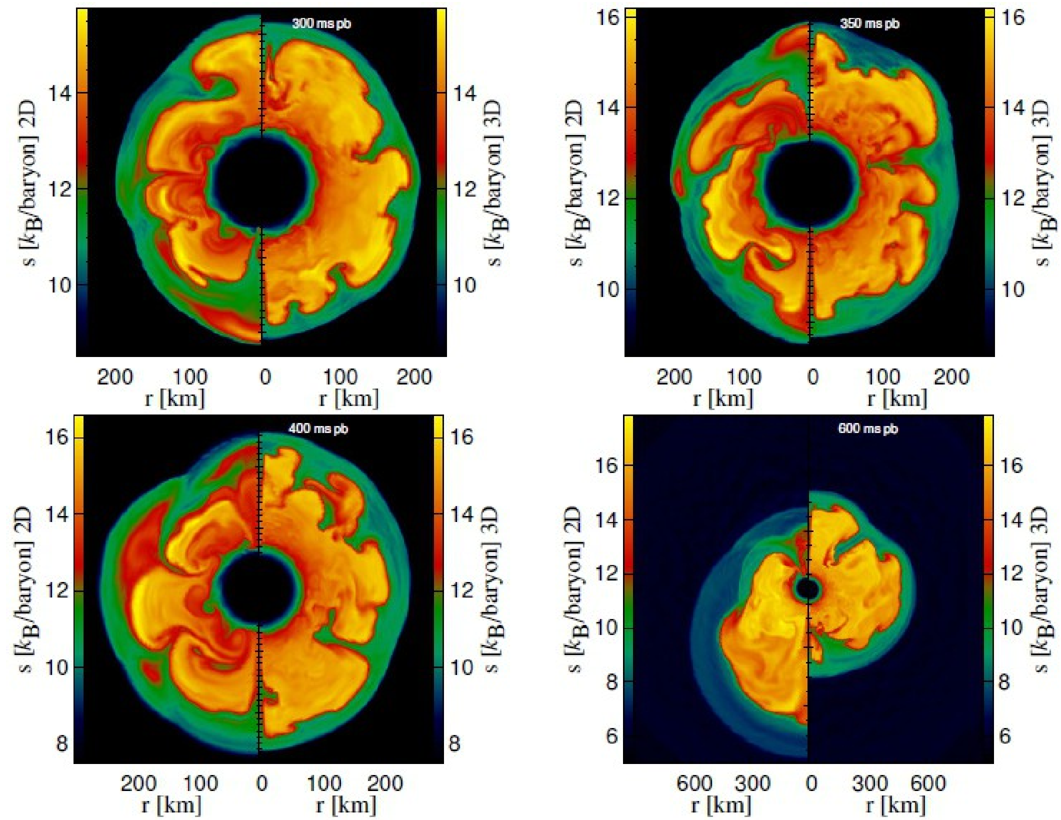

2D & 3D slices for 11.2 M_{sun} model, L = 1.0*10^{52} erg/s

2D-3D Differences

Average entropy of gas in gain layer is not good diagnostic quantity for proximity to explosion

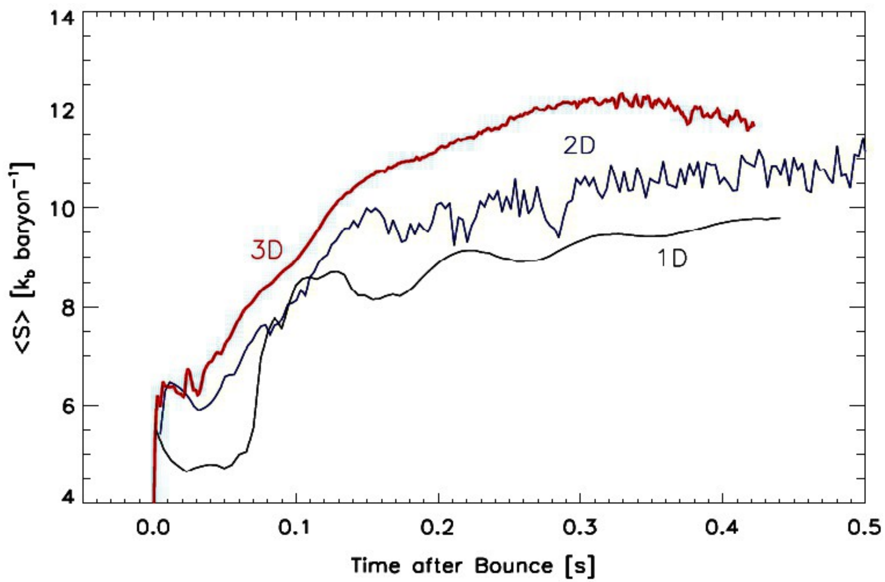

Nordhaus et al., ApJ 720 (2010) 694

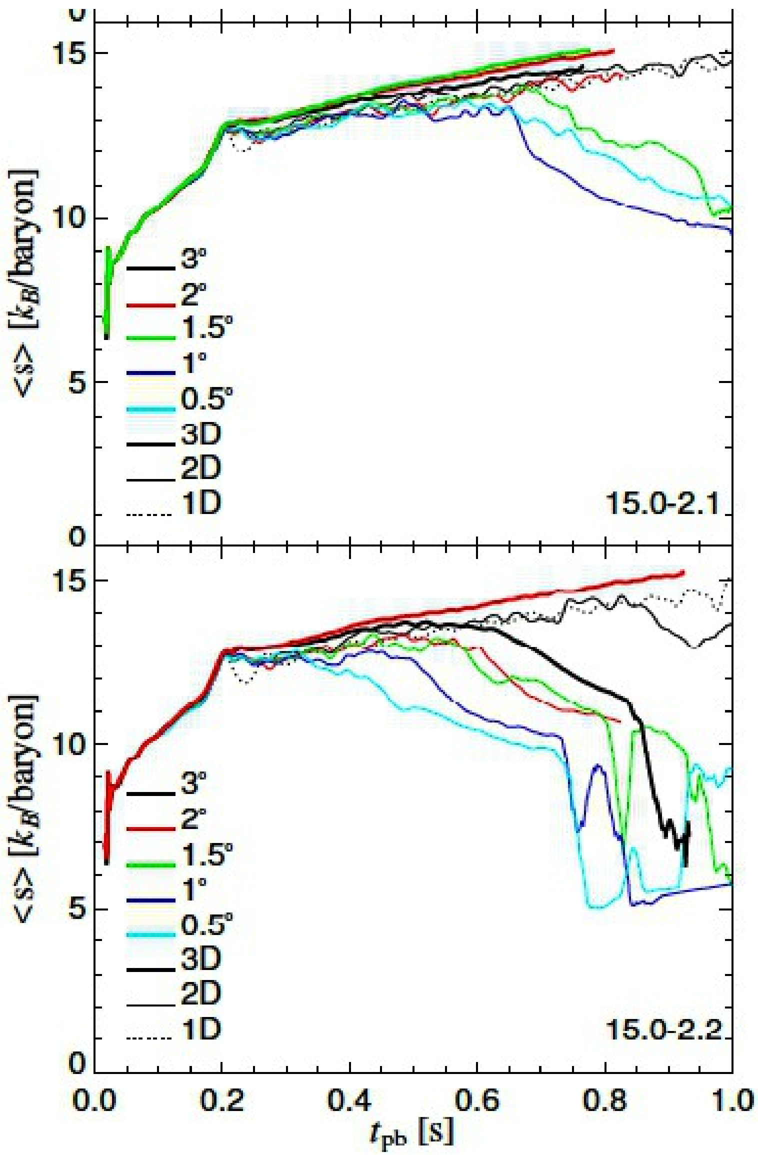

Hanke et al., ApJ 755 (2012) 138, arXiv:1108.4355

Growing "Diversity" of 3D Results

- Dolence et al. (arXiv:1210.5241) find much smaller 2D/3D difference of critical luminosity but still somewhat earlier explosion in 3D. Confirm that entropy does not indicate readiness to explosion and deny importance of SASI in 3D. Is longer dwell time of mass in gain layer cause for result?
- Takiwaki et al. (ApJ 749:98, 2012) obtain explosion for an 11.2 M_{sun} progenitor in 3D later than in 2D. See differences in convection inside the proto-NS and slightly faster 3D explosions with higher resolution.
- Couch (arXiv:1212.0010) finds also faster explosions in 2D than in 3D and somewhat higher critical luminosity in 3D ! But critical luminosity increases in 2D with higher resolution, but no high-resolution 3D case!
- Ott et al. (arXiv:1210.6674) reject relevance of SASI in 3D but diagnose dominance of neutrino-driven convection. Yet, they confess that result may be affected by large perturbations associated with cartesian grid.
- Kuroda et al. (ApJ 755: 11, 2012) confirm relevance of general relativistic gravity in 3D, supporting previous results in 1D and 2D; however, no comparison of 2D vs. 3D was made.

Growing "Diversity" of 3D Results

- These results do not yield a clear picture of 3D effects.

  But:

- The simulations were performed with different grids (cartesian+AMR, polar), different codes (CASTRO, ZEUS, FLASH, Cactus, Prometheus), and different treatments of input physics for EOS and neutrinos, some with simplified, not fully self-consistent set-ups.
- Resolution differences are difficult to assess and are likely to strongly depend on spatial region and coordinate direction.
- Partially compensating effects of opposite influence might be responsible for the seemingly conflicting results.
- Convergence tests with much higher resolution and detailed code comparisons for "clean", well defined problems are urgently needed, but both will be ambitious!

A Comment on SASI in SN Cores

- SASI growth is well understood, analytically, numerically, and experimentally (see SWASI analog).
- SASI triggers convection and SASI amplitudes saturate by parasitic instabilities
- Neutrino-driven convection affects SASI, whether supportive (by pumping energy) or suppressive (by destroying mode coherence) is presently not clear.
- SASI grows preferentially in fast accretion flows, in which neutrino-driven convection is hampered ($t_{adv}/t_{conv} < 3$ ===> growth of neutrino-driven convection is suppressed; Foglizzo et al. ApJ 2006).
- Dominance of SASI or convection is likely to depend on progenitor and phase of post-bounce evolution.
- SASI might play important role in 3D despite potentially smaller amplitude. What is role of spiral SASI in rotating stellar cores?

Laboratory Astrophysics

"SWASI" Instability as an analogue of SASI in the supernova core

Foglizzo et al., PRL 108 (2012) 051103

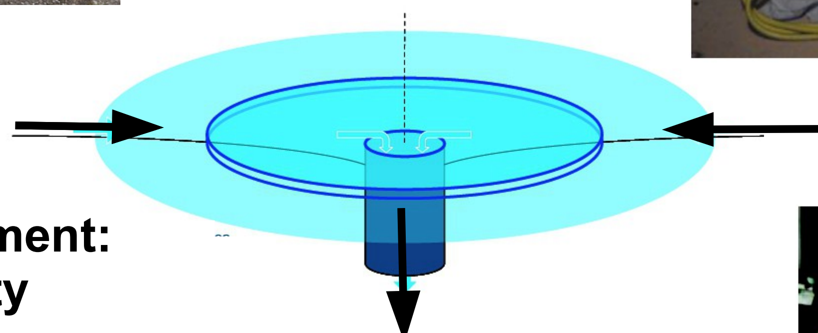

Constraint of experiment:
No convective activity

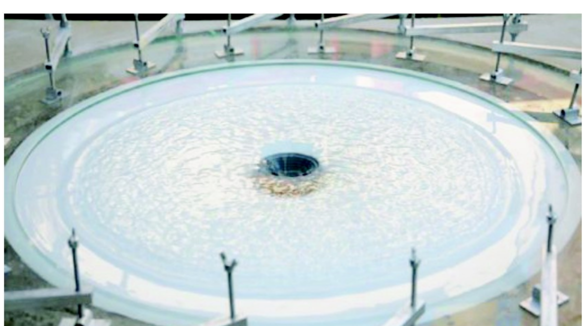

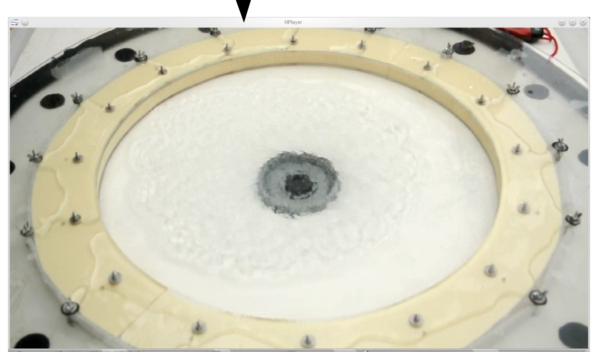

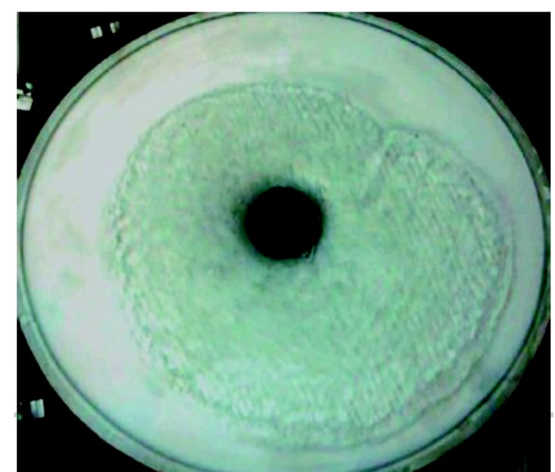

Summary

- Modelling of SN explosion mechanism has made considerable progress in 1D and multi-D.
- 2D relativistic models yield explosions for "soft" EoSs. Explosion energy tends to be on low side (except, maybe, recent models by Bruenn et al., arXiv:1212.1747).
- 3D modeling has only begun. No clear picture of 3D effects yet.
- 3D SN modeling is extremely challenging and variety of approaches for neutrino transport and hydrodynamics/grid choices will be and need to be used.
- Numerical effects (and artifacts) and resolution dependencies in 2D and 3D models must still be understood.
- Bigger computations on faster computers are indispensable, but higher complexity of highly-coupled multi-component problem will demand special care and quality control.